

Full Length Article

A comparative analysis of modeling and solution methods for the en-route charging station location problems within uncongested and congested highway networks

Xueqi Zeng^a, Chi Xie^{a,b,c,*}^a Urban Mobility Institute, Tongji University, China^b Key Laboratory of Road and Traffic Engineering of Ministry of Education, Tongji University, China^c School of Transportation Engineering, Tongji University, China

ARTICLE INFO

Keywords:

Electric vehicles
Charging station location problems
Metanetworks
Bi-level programming models
Branch-and-bound algorithm

ABSTRACT

This paper investigates a widely discussed class of charging station location problems for the en-route charging need of electric vehicles traveling in intercity highway networks. Due to the necessity for multiple charges along an intercity long-haul trip, this type of charging station location problems implies such an individual behavior that electric vehicle drivers make self-optimal route-and-charge decisions while ensuring the driving range of their vehicles to sustain trips without running out of charge. The main contribution of this paper is on analytically and computationally comparing the modeling and solution methods for the charging station location problems within uncongested and congested networks. Two distinct modeling frameworks are presented and analyzed: A metanetwork-based two-stage model for uncongested networks and a network-based bi-level model for congested networks. Both models are tackled by the classic branch-and-bound algorithm, which, however, resorts to different problem decomposition schemes, subregion bounding strategies, and network flow evaluation methods. Specifically, for uncongested networks, a two-phase procedure first employs a bi-criterion label-correcting algorithm for constructing a metanetwork and then implements the branch-and-bound algorithm on the metanetwork embedding a single-criterion label-setting algorithm for deriving network flows; on the other hand, for congested networks, the branch-and-bound algorithm is directly applied on the original network encapsulating a convex combinations method for deriving network flows. Finally, the two network scenarios and their modeling and solution methods are quantitatively evaluated with two real-world highway networks, in terms of implementation complexity, solution efficiency, and routing behavior.

1. Introduction

1.1. Background

The intensifying concerns over the energy crisis and the escalating impact of global warming highlight the urgent need for a shift away from dependence on fossil fuels toward renewable energy sources. Within the transportation sector, a crucial facet of this transition involves the widespread adoption of renewable energy vehicles, especially electric vehicles powered by onboard batteries (Wang et al., 2018). However, despite the implementation of various governmental initiatives aimed at promoting public acceptance of

* Corresponding author at: 4800 Cao'an Hwy., Shanghai 201804, China.

E-mail address: chi.xie@tongji.edu.cn (C. Xie).

<https://doi.org/10.1016/j.mutra.2024.100150>

Received 14 February 2024; Received in revised form 4 April 2024; Accepted 20 April 2024

2772-5863/© 2024 The Author(s). Published by Elsevier Ltd on behalf of Southeast University. This is an open access article under the CC BY-NC-ND license (<http://creativecommons.org/licenses/by-nc-nd/4.0/>)

electric vehicles, their adoption rates remain surprisingly low. According to the statistics from the [International Energy Agency \(2020\)](#), as of 2019, electric vehicle sales accounted for merely 2.6% of the global automotive market, with electric vehicles accounting for a mere 1% of the total global vehicle stock.

One significant obstacle impeding the widespread adoption of electric vehicles is the phenomenon known as “range anxiety” among electric vehicle drivers ([Kassakian, 2013](#)). This term encapsulates the worry that electric vehicle drivers feel regarding the limited driving range of their vehicles and the possibility of the battery depleting before reaching a destination or a charging station ([Franke and Krems, 2013](#)). Across numerous major cities globally, the driving range of electric vehicles is typically sufficient for daily commutes ([Pearre et al., 2011](#); [Stark et al., 2015](#); [Shi et al., 2019](#)). However, during intercity long-distance trips, electric vehicles may require multiple charging stops along the path due to their limited driving range. In this situation, electric vehicle drivers may suffer range anxiety.

Generally, increasing en-route charging opportunities for electric vehicles proves to be a highly effective method in alleviating or eradicating range anxiety ([Pearre et al., 2011](#)). Nevertheless, the construction of charging stations is both time and cost-intensive ([Xu et al., 2020](#)), making it impractical to install them at every potential location. On the other hand, an imbalanced distribution of charging stations may compel electric vehicles to deviate from their shortest paths for charging, resulting in extended travel times for electric vehicle travelers over the network. Consequently, optimizing the locations of these en-route charging stations within intercity highway networks becomes crucial.

1.2. Related studies

In recent years, electric vehicle charging station location problems have drawn substantial attention from researchers in various academic disciplines. A comprehensive review that delves into mathematical models and solution algorithms for charging station location problems is due to [Kchaou-Boujelben \(2021\)](#). This review offers a classification system and a comparative assessment of related research endeavors. Moreover, [Shen et al. \(2019\)](#) provided an exhaustive review focusing on the location and operation problems of charging stations for electric vehicles. Given the focus of this paper on a comparison of modeling and solution methods for charging station location problems in uncongested and congested networks, we set the following review work into two categories: (1) Optimal en-route charging station location problems for uncongested networks; (2) optimal en-route charging station location problems for congested networks.

1.2.1. Uncongested networks

Within uncongested networks, the cost/time with each link is given as a constant, independent on the link flow. In terms of objective functions, the optimization models in this category can be subdivided into two subcategories: (1) Maximizing (charging) demands that are satisfied or covered, and (2) minimizing various costs.

The pioneering efforts in facility location models of maximizing demands can be traced back to [Hodgson \(1990\)](#) and [Berman et al. \(1992\)](#), where the flow capturing location model (FCLM) and the flow intercepting location model (FILM) were introduced, respectively. These models aim to identify optimal service facility locations to maximize captured or intercepted customer flows within traffic networks. Subsequent research by [Hodgson and Rosing \(1992\)](#) and [Hodgson et al. \(1996a, 1996b\)](#) expanded on FCLM, but these models overlooked vehicle driving range constraints. To address this issue, [Kuby and Lim \(2005\)](#) proposed the flow refueling location model (FRLM) to maximize vehicles that are refueled within traffic networks, where vehicles require refueling multiple times during a trip. Additionally, [Kuby and Kim \(2007\)](#) refined this approach, exploring methods wherein not all charging stations had to be exclusively located at network nodes. While the FRLM provides a comprehensive representation of electric vehicle charging demands, its computational complexity presents challenges in large-scale traffic networks. To mitigate this, some researchers proposed efficient heuristics ([Lim and Kuby, 2010](#); [Chung et al., 2018](#); [Tran et al., 2018](#)), while others developed novel mathematical models addressing maximal covering flow problems and offered more efficient solution methodologies than previous models ([Capar et al., 2013](#); [MirHassani and Ebrazi, 2013](#)). On the basis of the original FRLM, several variants emerged, including the FRLM with charging station capacity constraints (CFRLM) ([Upchurch et al., 2009](#); [Wang and Lin, 2013](#); [Hosseini and MirHassani, 2015](#); [Hosseini et al., 2017](#)) and the FRLM with deviations (DFRLM) ([Kim and Kuby, 2012](#); [Kim and Kuby, 2013](#); [Hosseini et al., 2017](#); [Yildiz et al., 2016](#); [Kweon et al., 2017](#); [Arslan et al., 2019](#); [Göpfert and Bock, 2019](#); [Xu and Meng, 2020](#)). In DFRLM, drivers can deviate from the shortest or most cost-effective path to refuel their vehicles if adequate refueling stations along the path are unavailable.

The optimal charging station location problems of minimizing the system cost or maximizing the system profit constitutes another research direction, encompassing various requirements and features. Some consider charging station capacities ([Wang and Lin, 2009](#); [Ghamami et al., 2016](#); [Zheng and Peeta, 2017](#); [Zhang et al., 2018a](#); [Rose et al., 2020](#); [Fakhrmoosavi et al., 2021](#); [Kavianipour et al., 2021](#)), while others concentrate on the detour behavior of electric vehicles ([Li and Huang, 2014](#); [Zheng and Peeta, 2017](#); [Zhang et al., 2018a](#); [Fakhrmoosavi et al., 2021](#); [Li et al., 2022](#); [Zeng et al., 2024](#)). The cost components involved vary across these studies. Some studies primarily target minimizing total infrastructure investment ([Wang and Lin, 2009](#); [Li and Huang, 2014](#); [Zhang et al., 2015](#); [Ventura et al., 2017](#); [Zheng and Peeta, 2017](#); [Rose et al., 2020](#)), whereas others aim to minimize user costs, i.e., the sum of travel costs and recharging costs ([Wang, 2007](#); [Nourbakhsh and Ouyang, 2010](#); [Xylia et al., 2017](#); [Zhang et al., 2018a](#); [Li et al., 2022](#); [Zeng et al., 2024](#)). Additionally, several studies aim to minimize the total system cost, encompassing both infrastructure investment and user costs ([Ghamami et al., 2016](#); [Fakhrmoosavi et al., 2021](#); [Kavianipour et al., 2021](#); [Wang et al., 2023](#)).

For the sake of readers' convenience, we list all reviewed studies of charging station location problems within uncongested networks in [Table 1](#).

Table 1

An overview of studies of charging station location problems within uncongested networks.

Paper	Objective		Charging station capacity	Driving range	Detour behavior
	Maximize satisfied demand amount	Minimize system cost			
		User cost Investment cost			
Hodgson (1990)	✓				
Berman et al. (1992)	✓				
Hodgson and Rosing (1992)	✓				
Hodgson et al. (1996a; 1996b)	✓				
Kuby and Lim (2005)	✓			✓	
Kuby and Kim (2007)	✓			✓	
Upchurch et al. (2009)	✓		✓	✓	
Kim and Kuby (2012; 2013)	✓			✓	✓
Wang and Lin (2013)	✓		✓	✓	
Hosseini and MirHassani (2015)	✓		✓	✓	
Yildiz et al. (2016)	✓			✓	✓
Kweon et al. (2017)	✓			✓	✓
Hosseini et al. (2017)	✓		✓	✓	✓
Arslan et al. (2019)	✓			✓	✓
Göpfert and Bock (2019)	✓			✓	✓
Xu and Meng (2020)	✓			✓	✓
Wang (2007)		✓			
Wang and Lin (2009)			✓	✓	
Nourbakhsh and Ouyang (2010)		✓		✓	
Li and Huang (2014)			✓	✓	✓
Zhang et al. (2015)			✓	✓	
Ghamami et al. (2016)		✓	✓	✓	
Ventura et al. (2017)			✓	✓	
Xylia et al. (2017)		✓		✓	
Zheng and Peeta (2017)			✓	✓	✓
Zhang et al. (2018a)		✓	✓	✓	✓
Rose et al. (2020)			✓	✓	
Fakhrmoosavi et al. (2021)		✓	✓	✓	✓
Kavianipour et al. (2021)		✓	✓	✓	
Wang et al. (2023)		✓		✓	
Li et al. (2022)		✓		✓	✓
Zeng et al. (2024)		✓		✓	✓

1.2.2. Congested networks

In contrast, within congested networks, the cost/time with each link is flow-dependent. Studies falling within this category can be further classified into two subcategories according to their objectives: (1) Maximization of served charging/refueling demand, and (2) minimization of some networkwide cost (or combination of different networkwide costs).

There are only a few charging station location studies aiming to maximize charging/refueling demands in congested networks, termed the FCLM with the user equilibrium principle. For example, [Riemann et al. \(2015\)](#) investigated the optimal locations for wireless power transfer facilities for electric vehicles, aiming to maximize the captured traffic flow by these facilities within a network. Additionally, [He et al. \(2018\)](#) proposed a bi-level programming model that considered the driving range constraint of electric vehicles to maximize the usage of charging stations along various paths. Furthermore, [Wang et al. \(2018\)](#) developed a model for optimizing the location and capacity of fast charging stations in highway networks while adhering to construction budget constraints.

Conversely, a significant body of research is dedicated to locating en-route charging stations for electric vehicles within congested traffic networks, aiming to minimize a diverse range of costs. Some researchers examined the influence of charging station capacities on their optimal locations ([Chen et al., 2016](#)), while others incorporated drivers' deviation behaviors into their models ([He et al., 2013](#); [He et al., 2015](#); [Liu and Wang, 2017](#); [Zheng et al., 2017](#); [Guo et al., 2018](#); [Zhang et al., 2018b](#); [Wang et al., 2019b](#)). There are also studies that considered both the charging station capacity and drivers' deviation behavior ([Chen et al., 2016](#); [Wang et al., 2019a](#); [Chen et al., 2020](#); [Ghamami et al., 2020](#)). Regarding cost components, most studies fall into two main categories: (1) Minimization of travel time/costs or charging expenses ([He et al., 2013](#); [He et al., 2015](#); [Chen et al., 2016](#); [Liu and Wang, 2017](#); [Zheng et al., 2017](#); [Guo et al., 2018](#); [Zhang et al., 2018b](#); [Wang et al., 2019a](#); [Wang et al., 2019b](#); [Chen et al., 2020](#); [Ghamami et al., 2020](#)), and (2) minimizing the investment costs for building charging infrastructures ([He et al., 2013](#); [Guo et al., 2018](#); [Wang et al., 2019b](#); [Chen et al., 2020](#); [Ghamami et al., 2020](#)). Some researchers also aim to minimize trip failure costs ([He et al., 2015](#); [Liu and Wang, 2017](#)) or greenhouse emissions ([Zhang et al., 2018b](#)).

To provide readers with an overview of the relevant research, we list all reviewed studies of charging station location problems within congested networks in [Table 2](#).

Table 2

An overview of studies of charging station location problems within congested networks.

Paper	Objective					Charging station capacity	Driving range	Detour behavior
	Maximize satisfied demand	Minimize system cost						
		User cost	Investment cost	Trip failure cost	Carbon emissions			
Riemann et al. (2015)	✓						✓	✓
He et al. (2018)	✓						✓	✓
Wang et al. (2018)	✓					✓	✓	✓
He et al. (2013)		✓	✓					
He et al. (2015)		✓		✓			✓	✓
Chen et al. (2016)		✓				✓	✓	✓
Liu and Wang (2017)		✓		✓			✓	✓
Zheng et al. (2017)		✓					✓	✓
Guo et al. (2018)		✓	✓				✓	✓
Zhang et al. (2018b)		✓				✓	✓	✓
Wang et al. (2019a)		✓					✓	✓
Wang et al. (2019b)		✓	✓			✓	✓	✓
Chen et al. (2020)		✓	✓			✓		✓
Ghamami et al. (2020)		✓	✓			✓	✓	✓
Bao and Xie (2021)		✓					✓	✓

1.3. Contributions

From the above review work, we can see that a number of studies have defined, modeled and solved the optimal en-route charging station location problems for electric vehicles in congested and uncongested networks. Nevertheless, an interesting question about modeling and solving this type of charging station location problems remains unanswered: How different are the modeling and solution methods used for a congested network from those for an uncongested network, if all the other settings (such as route-and-charge choice behavior, driving range perception, driving population composition, and so on) for the two problem versions are the same? Recent research advances for the optimal en-route charging station location problem for uncongested networks present a very efficient modeling and solution framework. However, it is not clear whether this framework is suitable for the problem for congested networks.

To answer this question, the modeling and solution methods for the en-route charging station location problems for uncongested networks and congested networks will be presented side by side and their differences will be analyzed and evaluated in a comparative manner. We believe that such an analytical and numerical comparison occurs for the first time in this field and the insights and lessons from studying and comparing these two problem versions may be very useful for methodological development and selections when we model and solve other types of charging station location problems or even general facility location problems for transportation networks, when traffic congestion arises as a modeling concern.

The subsequent sections of this paper follow such a structure: [Section 2](#) defines the en-route charging station location problem and constructs two mixed integer programming models for the uncongested and congested network cases. The common part of these two models is maximally kept while their differences are emphasized and comparatively analyzed: A metanetwork-based two-stage model for uncongested networks and a network-based bi-level model for congested networks. By utilizing these different model structures, [Section 3](#) accordingly proposes and compares two different solution algorithm frameworks, both of which employ the branch-and-bound strategy but their algorithmic implementations are distinct and exhibit different solution convergence rates. In [Section 4](#), the application of these methods for a real-world highway network is detailed, validating and affirming their effectiveness and efficiency difference. Finally, [Section 5](#) concludes this paper by offering remarks and suggesting potential avenues for future research.

2. Problem formulations

2.1. Problem statement and modeling assumptions

The en-route charging station location problem addressed in this study falls into the category of facility location problems. Specifically, it focuses on an intercity highway network comprising nodes (such as cities or interchanges) and links (highway segments), with travelers operating EVs in this network. When the driving range of EVs is insufficient to cover the physical length of the minimum-cost path (e.g., based on time or monetary cost), EV drivers must charge en-route once or more times. This often necessitates detours for charging, thereby increasing their travel costs. Under these circumstances, constrained by the budget limit on charging station construction, this paper seeks to identify optimal charging station locations among candidate nodes for constructing charging stations. The objective is to minimize the total travel cost of EV drivers while ensuring that all EV drivers can complete their trips relying on their vehicles, whether with or without en-route charging.

Without loss of generality, several commonly used assumptions are proposed for both charging station location problems for uncongested and congested networks:

- (1) For simplicity, this paper assumes that all electric vehicle drivers make route-and-charge choices in a self-optimal manner with the same driving range limit. Here the homogeneous driving range setting could be readily relaxed if needed (see, [Xie et al., 2017](#), for example).
- (2) It is assumed that with a specified construction budget limit, at least one feasible solution exists for the problem, whether in uncongested or congested networks. If necessary, the trip failure situation can be easily incorporated into our models (see, [Zeng et al., 2024](#), for example).
- (3) The relationship between the energy consumption and driving distance of electric vehicles is assumed to be proportional, as used by many previous researchers in the literature ([Xie and Jiang, 2016](#); [Ghamami et al., 2020](#); [Zeng et al., 2024](#)). Recently, [Donkers et al. \(2020\)](#) confirmed the nearly linear relationship between driving distance and energy consumption.
- (4) The models do not encompass charging costs such as charging fees and charging time, as used by many previous researchers in the literature ([Xie and Jiang, 2016](#); [Xie et al., 2017](#); [Bao and Xie, 2021](#); [Li et al., 2022](#); [Zeng et al., 2024](#)). This exclusion is based on observations suggesting that drivers prioritize driving range satisfaction over charging costs ([Lin and Greene, 2011](#); [Ge and MacKenzie, 2022](#)). While charging and waiting times contribute to total travel time and influence routing behavior in specific cases, their impact is relatively marginal compared to the overall travel time of intercity long-haul trips.
- (5) It is assumed that electric vehicles are fully charged at both their origins and en-route charging stations. This widely used assumption ([Xie and Jiang, 2016](#); [Bao and Xie, 2021](#); [Li et al., 2022](#); [Zeng et al., 2024](#)) is based partly on the preparation habits of electric vehicle travelers planning intercity long-haul trips and partly on the exclusion of any charging costs within our model.

These assumptions, particularly the last two, present an idealized and simplified condition that might not fully align with real-world behavioral complexity. However, these settings do not significantly distort the real route-and-charge behavior and greatly reduce the modeling complexity.

2.2. Notation

Let us define a set of nodes in a general highway network, denoted by N , and a set of links in the highway network, represented by A , where $i, j \in N$ and $(i, j) \in A$. Additionally, a subset of N , denoted by L , represents the set of candidate nodes for constructing charging stations. Furthermore, the set $W = \{(r, s)\}$ contains all the O-D pairs, where r and s represent the origin node and the destination node, respectively. We also introduce an essential set, K_{rs} , which denotes the set of all paths connecting O-D pair (r, s) .

For additional clarity, please refer to [Tables 3–5](#), which provide a comprehensive list of notations used in the modeling process of the two problems.

In addition to the assumptions and notations mentioned above, several network modeling components will be utilized in our model, formally defined as follows:

Definition 1 (Subpath): A subpath represents a continuous arc that connects certain links on path k from r to s , where both the head and tail nodes of this arc are charging station nodes ([Xie and Jiang, 2016](#)). Illustrated in [Fig. 1](#) where r, u, v , and s are charging station nodes, six subpaths are identifiable: $k^{rs,ru}$, $k^{rs,uv}$, $k^{rs,us}$, $k^{rs,rv}$, $k^{rs,us}$, and $k^{rs,rs}$.

Definition 2 (Feasible subpath): A subpath is considered feasible for travelers if its length does not surpass their driving ranges. This implies that feasible subpaths for travelers with different driving ranges might be different. For example, in [Fig. 1](#), assuming

Table 3

Common notation for the two problems for uncongested and congested networks.

Sets	Definition
N	Set of nodes, $i, j \in N$
L	Set of candidate nodes for charging stations, $l \in L$
A	Set of links, $(i, j) \in A$
W	Set of O-D pairs, $(r, s) \in W$
K_{rs}	Set of paths from origin r to destination s
Parameters	Definition
G	Budget limit for constructing charging stations
D	Driving range of electric vehicles
M	A sufficiently large constant
e_l	Investment cost for constructing a charging station at node l , where $l \in L$
g_{rs}	Travel demand rate from r to s
d_{ij}	Physical length of link (i, j)
Variables	Definition
z_l	Binary decision variable with a value of 1 if a charging station is built at node l and with a value of 0 if otherwise
f_k^{rs}	Traffic flow rate on path k from r to s

Table 4

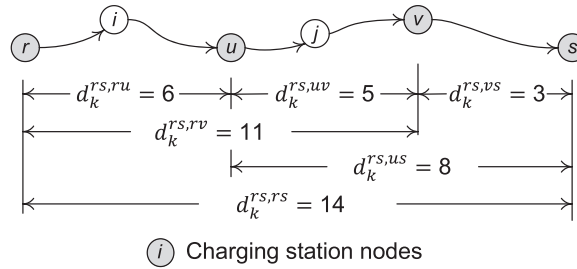
Notation specific to the problem for uncongested networks.

Sets	Definition
H	Set of pure feasible subpaths with the minimum cost between any two charging station nodes u and v , where $h_{uv} \in H$
Parameters	Definition
c_{ij}	Travel cost of link (i, j) in uncongested highway networks
$\delta_k^{rs,uv}$	Minimum-cost feasible subpath-path incidence indicator in uncongested highway networks, which equals 1 if the minimum-cost feasible subpath between u and v is a part of path k from r to s and equals 0 if otherwise
Variables	Definition
f_{uv}	Traffic flow rate on the minimum-cost feasible subpath k_{uv} between u and v in uncongested highway networks
f_{ij}	Binary activation indicator of link (i, j) in uncongested highway networks, the value of which equals 1 if this link is a part of the minimum-cost feasible subpath between u and v and equals 0 if otherwise

Table 5

Notation specific to the problem for congested networks.

Sets	Definition
U_k^{rs}	Set of charging station node pairs (u, v) on path k from r to s in congested highway networks, where $(u, v) \in U_k^{rs}$
Parameters	Definition
$c_{0,ij}$	Free-flow travel cost of link (i, j) in congested highway networks
v_{ij}	Capacity of link (i, j) in congested highway networks
α_{ij}, β_{ij}	Parameters in the travel cost function of link (i, j) in congested highway networks
$\delta_{ij,k}^{rs}$	Link-path incidence indicator in congested highway networks, which equals 1 if path k from r to s covers link (i, j) and equals 0 if otherwise
$d_k^{rs,uv}$	Physical length of subpath (u, v) on path k from r to s in congested highway networks, which equals the sum of the length of links in this subpath
$\delta_{ij,k}^{rs,uv}$	Link-subpath incidence indicator in congested highway networks, which equals 1 if subpath (u, v) on path k from r to s traverses link (i, j) and equals 0 if otherwise
Variables	Definition
x_{ij}	Traffic flow rate on link (i, j)
y_k^{rs}	Binary activation indicator of path k between O-D pair (r, s) , where if $y_k^{rs} = 1$, i.e., path k between O-D pair (r, s) is active, $f_k^{rs} \geq 0$, and if y_k^{rs} equals 0, $f_k^{rs} = 0$
$y_k^{rs,uv}$	Binary activation indicator of subpath (u, v) on path k between O-D pair (r, s) , where if $d_k^{rs,uv} > D$, i.e., subpath (u, v) on path k between O-D pair (r, s) is infeasible for travelers, $y_k^{rs,uv} = 0$, and if otherwise, $y_k^{rs,uv}$ equals 0 or 1
$c_{ij}(x_{ij})$	Travel cost of link (i, j) in congested highway networks, which is dependent on the link flow rate x_{ij}

**Fig. 1.** An illustration of the subpath.

a driving range of 12, feasible subpaths include $k^{rs,ru}$, $k^{rs,uv}$, $k^{rs,vs}$, $k^{rs,rv}$, and $k^{rs,us}$. Conversely, with a driving range of 6, feasible subpaths include only $k^{rs,ru}$, $k^{rs,uv}$, and $k^{rs,vs}$.

Definition 3 (Feasible path): A path is defined as feasible if at least a group of continuous feasible subpaths can be found to precisely cover it. The minimum driving range that renders a path feasible is termed the critical driving range of the path.

Definition 4 (Pure subpath): Derived from subpaths, if a subpath $k^{rs,uv}$ solely comprises nodes u and v as charging station nodes, we define it as a pure subpath. For instance, in Fig. 1, there are three pure subpaths: $k^{rs,ru}$, $k^{rs,uv}$, and $k^{rs,vs}$.

Definition 5 (Minimum-cost feasible subpath): A feasible subpath, denoted as $k^{rs,uv}$, connecting charging station nodes u and v along path k between O-D pair (r, s) , is termed the minimum-cost feasible subpath connecting u and v if the cost of $k^{rs,uv}$ is the minimum among all such feasible subpaths, i.e., $c_k^{rs,uv} = \min_{(r',s') \in W, h \in H_{r',s'}} c_h^{r's',uv}$, where $c_h^{r's',uv}$ is the travel cost of subpath $h^{r's',uv}$. Here, $h^{r's',uv}$ implies the subpath that connects nodes u and v on path h between O-D pair (r', s') .

Definition 6 (Station-subpath metanetwork): A station-subpath metanetwork $G^M = (N^M, A^M)$ can be created from the original node-link traffic network (N, A) . In the metanetwork, the nodes in N^M comprise all charging station nodes, along with origin and

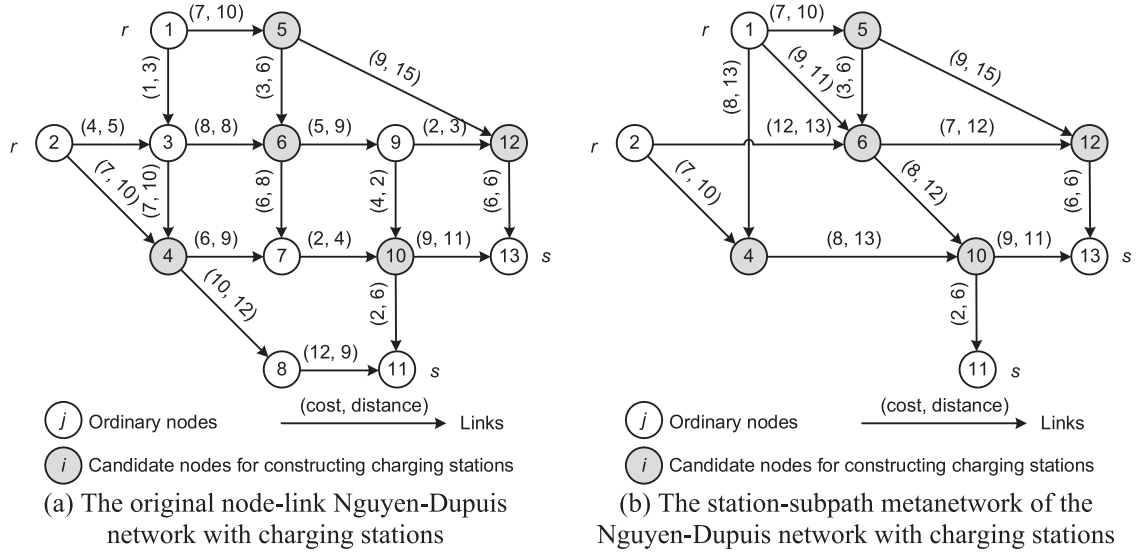


Fig. 2. Illustration of the construction of the station-subpath metanetwork from an original node-link network.

destination nodes extracted from the node-link traffic network, where $N^M \subseteq N$. Any link within set A^M represents a minimum-cost feasible subpath connecting a pair of charging station nodes (or an origin/destination node and a charging station node, or an origin node and a destination node) in the node-link network, whenever such a subpath exists and is a pure subpath, where $A^M \subseteq N^M \times N^M$. For example, we employ a simple traffic network, the Nguyen-Dupuis network, to demonstrate the establishment of the station-subpath metanetwork. Fig. 2(a) displays the original Nguyen-Dupuis network in the node-link form, encompassing the network's topology, link attributes, charging station locations, and O-D pairs. Assuming a driving range of $D = 15$, the station-subpath metanetwork for the Nguyen-Dupuis network can be formulated as depicted in Fig. 2(b). In this instance, the original node-link Nguyen-Dupuis network comprises 13 nodes and 19 links, whereas its station-subpath metanetwork consists of only 9 nodes and 13 links. Evidently, compared to the original node-link network, the station-subpath metanetwork features a reduced number of nodes and links, thereby potentially diminishing the problem size and computational complexity when employing a network optimization algorithm.

2.3. A metanetwork-based two-stage model for uncongested networks

Based on Definition 3 and Definition 5, and considering the assumption that travelers consistently opt for the feasible path with the minimum cost, for any chosen path by travelers, if it covers two charging station nodes u and v , the subpath between u and v on this path must be the minimum-cost feasible subpath between nodes u and v . The cost of this subpath is $c_{uv}^* = \min_{(r,s) \in W, k \in K_{rs}} c_k^{rs,uv}$. Hence, if these minimum-cost feasible subpaths can be predetermined, it becomes possible to circumvent the extensive and repetitive computations required for establishing the specific track from u to v for every minimum-cost feasible path k , $k \in K_{rs}$, $(r, s) \in W$.

Moreover, in uncongested networks, the fixed travel cost of each link signifies that the cost of each subpath remains fixed, which makes it possible to derive all minimum-cost feasible subpaths connecting any two charging station nodes. Under this circumstance, travelers' chosen paths can be depicted as a sequence of charging station nodes and a sequence of minimum-cost feasible subpaths connecting these nodes. Consequently, this approach helps circumvent a large number of repeated path-finding operations while directly invoking the minimum-cost feasible subpath from the station-subpath metanetwork when needed (Li et al., 2022).

Based on the preceding analysis, determining the minimum-cost feasible subpaths between two charging station nodes, or an origin/destination node and a charging station node, or an origin and a destination node, denoted as (u, v) , equates to constructing the station-subpath metanetwork. For each (u, v) in the node-link network, we formulate an integer programming model presented as follows:

$$c_{uv}^* = \min_{\{f_{ij}\}} \sum_{(i,j) \in A} c_{ij} f_{ij} \quad (1)$$

$$\text{subject to } \sum_{\{j:(i,j) \in A\}} f_{ij} - \sum_{\{j:(j,i) \in A\}} f_{ji} = \begin{cases} 1 & i = u \\ 0 & i \in N \setminus \{u, v\} \\ -1 & i = v \end{cases} \quad (2)$$

$$\sum_{(i,j) \in A} d_{ij} f_{ij} \leq D \quad (3)$$

$$f_{ij} \in \{0, 1\} \quad \forall (i, j) \in A \quad (4)$$

where the objective function described in Eq. (1) aims to minimize the sum of travel costs of active links, in other words, minimizing the cost of the subpath. Furthermore, Eq. (2) delineates the flow conservation constraints applicable to the origin node, other nodes excluding both origin and destination nodes, and the destination node of the subpath, respectively. Additionally, Eq. (3) ensures that the cumulative length of all active links, i.e., the length of the subpath, does not exceed travelers' driving range, thus ensuring the feasibility of the subpath. Lastly, Eq. (4) symbolizes the activation indicator of each link as a binary variable.

The aforementioned model enables the determination of the minimum-cost feasible subpath between nodes u and v , whose cost is denoted by c_{uv}^* . Once this subpath is recognized as a pure subpath, it becomes part of H , the set of pure feasible subpaths with the minimum cost. By precomputing all minimum-cost feasible subpaths, the construction of the station-subpath metanetwork is an easy task.

From the perspective of the metanetwork, finding a minimum-cost path subject to the driving range constraint in the original network is equivalent to finding a minimum-cost path in the metanetwork. This problem can be represented through a linear programming model that determines the network flow pattern:

$$\min \sum_{\{(u,v)|h_{uv} \in H\}} c_{uv}^* f_{uv} \quad (5)$$

$$\text{subject to } \sum_{k \in K_{rs}} f_k^{rs} = g_{rs} \quad \forall (r, s) \in W \quad (6)$$

$$f_k^{rs} \geq 0 \quad \forall k \in K_{rs}, (r, s) \in W \quad (7)$$

$$f_{uv} = \sum_{(r,s) \in W} \sum_{k \in K_{rs}} \delta_k^{rs,uv} f_k^{rs} \quad \forall (u, v) \in \{(u, v) | h_{uv} \in H\} \quad (8)$$

$$f_{uv} \leq M z_u \text{ and } f_{uv} \leq M z_v \quad \forall (u, v) \in \{(u, v) | h_{uv} \in H\} \quad (9)$$

where the objective function presented in Eq. (5) aims to minimize the total travel costs across the metanetwork. In this function, $\{c_{uv}^*\}$ represents a parameter vector derived from solving the model depicted in Eqs. (1)–(4). Furthermore, Eq. (6) encompasses the flow conservation constraints applicable to each O-D pair. Meanwhile, Eq. (7) ensures the non-negativity of the path flow rate. Eq. (8) establishes the relationship between flow rates on subpaths and on paths. Eq. (9) indicates the definition of a subpath, i.e., there are charging stations at the head node and the tail node of a subpath.

Subsequently, a mixed integer linear programming model is designed to minimize the total travel costs over the whole metanetwork and to identify the optimal locations for charging stations is expressed as follows:

min Eq. (5)

subject to Eqs. (6)–(9)

$$\sum_{l \in L} e_l z_l \leq G \quad (10)$$

$$z_l \in \{0, 1\} \quad \forall l \in L \quad (11)$$

where Eq. (10) ensures that the total investment costs for constructing charging stations do not exceed the specified budget limit. Additionally, Eq. (11) indicates that z_l is a binary variable.

Overall, in this metanetwork-based two-stage model, the first stage involves $|L\{r\}\{s\}|(|L\{r\}\{s\}| - 1)$ integer programming models presented in Eqs. (1)–(4), which helps the derivation of the cost vector $\{c_{uv}^*\}$ in Eq. (5) and the construction of the station-subpath metanetwork. Subsequently, in the second stage, a mixed integer linear programming model is presented in Eqs. (5)–(11) to find the optimal locations of charging stations for electric vehicles over the metanetwork.

2.4. A network-based bi-level model for congested networks

If traffic congestion is incorporated into the en-route charging station location problem, the travel cost of all or some links becomes flow-dependent. A simplified function usually used in practice to describe the relationship between the link travel cost and link flow rate is the function developed by the U.S. Bureau of Public Roads (1964), as shown in Eq. (12):

$$c_{ij}(x_{ij}) = c_{0,ij} \left[1 + \alpha_{ij} \left(\frac{x_{ij}}{v_{ij}} \right)^{\beta_{ij}} \right] \quad \forall (i, j) \in A \quad (12)$$

where α_{ij} and β_{ij} are the model parameters and typically equal 0.15 and 4, respectively.

Therefore, link costs are not fixed; rather, they depend on flow, leading to variations in the minimum-cost feasible subpaths with the flow patterns. Therefore, attempting to derive the minimum-cost feasible subpaths in advance becomes futile because these subpaths may alter with changes in network flows. As a result, employing the metanetwork-based two-stage model becomes inappropriate in

congested networks. In response, a network-based bi-level model is developed to characterize the optimal charging station location problem for electric vehicles in congested networks.

Initially, we introduce a model addressing the equilibrium flow pattern within congested highway networks, as demonstrated below:

$$\min \sum_{(i,j) \in A} \int_0^{x_{ij}} c_{ij}(\tau) d\tau \quad (13)$$

$$\text{subject to } d_k^{rs,uv} = \sum_{(i,j) \in A} \delta_{ij,k}^{rs,uv} d_{ij} \quad \forall (u,v) \in U_k^{rs}, k \in K_{rs}, (r,s) \in W \quad (14)$$

$$d_k^{rs,uv} y_k^{rs,uv} \leq D \quad \forall (u,v) \in U_k^{rs}, k \in K_{rs}, (r,s) \in W \quad (15)$$

$$y_k^{rs,uv} \leq z_u \text{ and } y_k^{rs,uv} \leq z_v \quad \forall (u,v) \in U_k^{rs}, k \in K_{rs}, (r,s) \in W \quad (16)$$

$$y_k^{rs,uv} \in \{0, 1\} \quad \forall (u,v) \in U_k^{rs}, k \in K_{rs}, (r,s) \in W \quad (17)$$

$$\delta_{ij,k}^{rs} y_k^{rs} = \sum_{(u,v) \in U_k^{rs}} \delta_{ij,k}^{rs,uv} y_k^{rs,uv} \quad \forall k \in K_{rs}, (r,s) \in W \quad (18)$$

$$y_k^{rs} \in \{0, 1\} \quad \forall k \in K_{rs}, (r,s) \in W \quad (19)$$

$$f_k^{rs} \leq M y_k^{rs} \quad \forall k \in K_{rs}, (r,s) \in W \quad (20)$$

Eqs. (6)–(7)

$$x_{ij} = \sum_{(r,s) \in W} \sum_{k \in K_{rs}} \delta_{ij,k}^{rs} f_k^{rs} \quad \forall (i,j) \in A \quad (21)$$

The objective function expressed in Eq. (13) is Beckmann's transformation (Beckmann et al., 1956). The constraints specified in Eqs. (14)–(17) signify the subpath feasibility conditions. Specifically, Eq. (14) defines the interrelation between the physical lengths of subpaths and of links. Additionally, Eq. (15) stipulates the feasibility of a subpath based on its length not surpassing the driving range of travelers. Moreover, Eq. (16) ascertains the definition of a subpath that there are charging stations at both its head node v and tail node u . Lastly, Eq. (17) prescribes the binary nature of subpath activation indicators. Furthermore, constraints in Eqs. (18)–(19) outline the path feasibility criteria. Specifically, Eq. (18) ensures that for an active path, denoted as k , i.e., $y_k^{rs} = 1$, each link (i,j) within it should be covered by precisely one active subpath of this path, while any link not included must not be covered by any active subpath of this path. This constraint guarantees non-overlapping coverage between distinct active subpaths within the active path and ensures the collective composition of these subpaths exactly represents the entirety of the path. Additionally, Eq. (19) stipulates that the path activation indicator, y_k^{rs} , adheres to a binary domain. Moreover, Eq. (20) enforces that the path flow rate, f_k^{rs} , can be positive only if the path activation indicator, y_k^{rs} , equals 1, where M is a sufficiently large constant. Lastly, Eq. (21) establishes the relationship between flow rates on links and paths.

Building upon the mathematical model outlined in Eqs. (6)–(7), (13)–(21), a network-based bi-level programming model for optimizing the locations of charging stations for electric vehicles in congested networks is expressed as follows:

$$\min \sum_{(i,j) \in A} x_{ij} c_{ij}(x_{ij}) \quad (22)$$

subject to Eqs. (10)–(11)

$$x_{ij} \in \operatorname{argmin} \sum_{(i,j) \in A} \int_0^{x_{ij}} c_{ij}(\tau) d\tau \quad \forall (i,j) \in A \quad (23)$$

subject to Eqs. (6)–(7), (14)–(21)

2.5. Comparison between the mathematical programming models for uncongested and congested networks

A comparative analysis of the metanetwork-based two-stage model and the network-based bi-level model is summarized in Table 6.

Proposition 1 (Total travel cost monotony with an additional charging station in uncongested networks). In uncongested networks, establishing a charging station at a node where no station exists in a current solution of charging station locations will either reduce or maintain the total travel cost.

Table 6

A comparison of modeling components of the two charging station location models for uncongested and congested networks

	A metanetwork-based two-stage model for uncongested networks	A network-based bi-level model for congested networks
Problem structure and number	First stage: $ L\{r\}\{s\} (L\{r\}\{s\} - 1)$ integer programming models; Second stage: A mixed integer linear programming model;	A mixed integer nonlinear programming model;
Network type	First stage: Node-link network; Second stage: Station-subpath metanetwork;	Node-link network;
Objective function	First stage: Minimizing all station-to-station subpath costs; Second stage: Minimizing the total travel cost over the entire network;	Lower level: Beckmann's transformation; Upper level: Minimizing the total travel cost over the entire network;

Proof. Considering the metanetwork-based two-stage model delineated in [Subsection 2.3](#), introducing a charging station at a node lacking one in the current charging station locations relaxes [Eq. \(9\)](#). Consequently, this adjustment results in a reduced or equivalent objective function value, representing the total travel costs. \square

Proposition 2 (Total travel cost monotony with an additional charging station in congested system-optimal networks). In congested networks, if the network flow pattern adheres to the system optimum principle rather than the user equilibrium principle, introducing a charging station at a node lacking one in an existing solution of charging station locations will lead to reduced or equivalent total travel costs.

Proof. Examining the network-based bi-level model proposed in [Subsection 2.4](#), when the system optimum principle governs the network flow pattern, the objective function in the lower level ([Eq. \(13\)](#)) should be replaced by the objective function in the upper level ([Eq. \(22\)](#)), collapsing the bi-level model into a single-level model. Under these circumstances, adding a charging station at a node where there is no charging station in the current solution results in a larger feasible region (i.e., [Eq. \(16\)](#) is relaxed), thereby leading to a decreased or at least identical objective function value representing the total travel costs. \square

Proposition 3 (Total travel cost monotony with an increased budget limit in both uncongested and congested networks). In both congested and uncongested networks, an increase in the budget limit leads to reduced or at least equivalent total travel costs.

Proof. Increasing the budget limit relaxes the budget limit constraint represented by [Eq. \(10\)](#). In the metanetwork-based model within uncongested networks, this relaxation either decreases or maintains an unchanged value for the objective function, specifically the total travel costs. Besides, within the network-based bi-level model in congested networks, [Eq. \(10\)](#) serves as constraints for the upper-level model. Relaxing this constraint results in either a decreased or unchanged value of the objective function of the upper-level model, particularly the total travel costs. \square

Proposition 4 (Total travel cost monotony with an increased driving range in uncongested networks). In uncongested networks, an increase in travelers' driving range results in reduced or at least equivalent total travel costs.

Proof. In uncongested networks, an extension of the driving range relaxes [Eq. \(3\)](#), leading to a reduction or at least no change in the objective function value in the integer programming model: c_{uv}^* , thereby resulting in a decreased or an unchanged value of the objective function in the metanetwork-based model, specifically the total travel costs. \square

Remark 1. In congested networks, the conclusions in Proposition 1 and in Proposition 4 do not necessarily hold due to the bi-level structure outlined in [Eqs. \(6\) and \(7\)](#), [\(10\) and \(11\)](#), [\(14–23\)](#). An additional charging station or increased driving range might lead to a lower, higher, or unchanged total travel cost when traffic congestion arises.

3. Solution algorithm

In this section, two algorithmic procedures in the branch-and-bound framework are presented to solve both the metanetwork-based two-stage model and the network-based bi-level model. In [Subsections 3.1 and 3.2](#), we first delve into the solution methods for the network flow problems respectively within uncongested and congested networks where charging station locations are given. Following this, the branch-and-bound framework is introduced in [Subsection 3.3](#) and applied to address the optimal charging station location problems for uncongested and congested networks, respectively. In [Subsection 3.4](#), a comparative analysis of these algorithms for the two problems is summarized.

3.1. A two-phase method of label-correcting and label-setting procedures for deriving network flows in uncongested networks

Addressing network flows in uncongested networks involves two phases:

- (1) Solving the integer programming model outlined in [Eqs. \(1\)–\(4\)](#) for each pair of nodes (u, v) to construct the station-subpath metanetwork.
- (2) Solving the metanetwork-based linear programming model presented in [Eqs. \(5\)–\(9\)](#).

3.1.1. A bi-criterion label-correcting algorithm in the first phase

The integer programming model presented in [Eqs. \(1\)–\(4\)](#) tackles a distance-constrained minimum-cost path problem. To capture the two critical attributes of each path: “distance feasibility” and “cost-effectiveness”, a label with two attributes, denoted as $l_j =$

(c_j, d_j) for each node $j \in N$, is devised. Here, c_j and d_j respectively denote the cost and distance from the origin node to node j . The task is to identify the label with the minimum value of c_j while simultaneously ensuring $d_j \leq D$, where D represents travelers' driving range.

For the sake of clarity, we define a few terms: (1) Pareto-optimal domination: Consider two labels $l_1 = (c_1, d_1)$ and $l_2 = (c_2, d_2)$, we assert that l_1 is dominated by l_2 in terms of c_1 and d_1 when $c_1 \geq c_2$, $d_1 \geq d_2$, and at least one attribute of l_2 , for instance, c_2 (or d_2), is strictly less than c_1 (or d_1). (2) Pareto-optimal labels: If within a set of labels, we cannot identify a pair where one label dominates the other, we name these labels as Pareto-optimal labels.

The algorithm starts by initializing the set of Pareto-optimal labels to $L_j = \{(c_{uj}, d_{uj})\}$ for each node j , where c_{uj} and d_{uj} represent the cost and physical length of the link connecting nodes u and j , respectively. If u and j are not connected in the traffic network, both values are set to infinity; if j is the origin node u , both values are set to zero. Subsequently, for every link (i, j) in the traffic network and every label $l_i = (c_i, d_i)$ in the set of Pareto-optimal labels of node i , generate a new label $(c_i + c_{ij}, d_i + d_{ij})$ and add it to the set of Pareto-optimal labels of node j . Then perform a Pareto-optimal dominance check on this label set. After that, verify whether each label is feasible, i.e., delete $l_j = (c_j, d_j)$ from the Pareto-optimal label set L_j of node j if $d_j > D$. The iteration would not terminate until either the set of Pareto-optimal labels of any node remains unchanged or this process has been conducted for $|N| - 1$ times, where $|N|$ represents the number of nodes in the network. Finally, for each node j , the label with the minimum c_j is the cost of the minimum-cost feasible path from the origin node u to node j . The sequence of nodes along this path can be obtained by backtracking through their associated predecessor nodes.

For a step-by-step process, please refer to Procedure 1. Note that this procedure identifies the minimum-cost feasible subpath between the origin node u and any node v . To create the metanetwork, this procedure needs to be iterated for each station/origin/destination node u .

Procedure 1 A bi-criterion label-correcting algorithm

Step 0: Initialization.

Initialize the iteration counter to $t := 0$.

For each node $j \in N$ do

Initialize the set of predecessor nodes to $\Pi_j^{(t)} := \{\pi_j^{(t)}\} := \{u\}$ and the set of labels to $L_j^{(t)} := \emptyset$.

If $j = u$ then

$L_j^{(t)} := L_j^{(t)} \cup \{l_j^{(t)}\}$, where $l_j^{(t)} = (0, 0)$.

Else if nodes u and j are connected then

$L_j^{(t)} := L_j^{(t)} \cup \{l_j^{(t)}\}$, where $l_j^{(t)} = (c_{uj}, d_{uj})$, c_{uj} and d_{uj} are respectively the cost and distance of the link connecting these two nodes.

Else

$L_j^{(t)} := L_j^{(t)} \cup \{l_j^{(t)}\}$, where $l_j^{(t)} = (+\infty, +\infty)$.

End if

End for

Step 1: Label update.

$t := t + 1$.

$L_j^{(t)} := L_j^{(t-1)}$, $\Pi_j^{(t)} := \Pi_j^{(t-1)}$.

For each link $(i, j) \in A$ do

For each label $l_i^{(t-1)} \in L_i^{(t-1)}$ do

If $(c_i^{(t-1)} + c_{ij}, d_i^{(t-1)} + d_{ij})$ is not dominated by any $l_j^{(t-1)}$ in $L_j^{(t-1)}$ then

$L_j^{(t)} := L_j^{(t)} \cup \{(c_i^{(t-1)} + c_{ij}, d_i^{(t-1)} + d_{ij})\}$, $\Pi_j^{(t)} := \Pi_j^{(t)} \cup \{i\}$.

If any $l_j^{(t)}$ in $L_j^{(t)}$ is dominated by $(c_i^{(t-1)} + c_{ij}, d_i^{(t-1)} + d_{ij})$ then

$L_j^{(t)} := L_j^{(t)} \setminus \{l_j^{(t)}\}$, $\Pi_j^{(t)} := \Pi_j^{(t)} \setminus \{\pi_j^{(t)}\}$.

End if

End if

If $d_j^{(t)} > D$, $\forall l_j^{(t)} \in L_j^{(t)}$ then

$L_j^{(t)} := L_j^{(t)} \setminus \{l_j^{(t)}\}$, $\Pi_j^{(t)} := \Pi_j^{(t)} \setminus \{\pi_j^{(t)}\}$.

End if

End for

End for

Step 2: Termination check.

If $t = |N| - 1$ or $L_j^{(t)} = L_j^{(t-1)}$ for any $j \in N$ then

For each node v do

$c_{uv}^* := \min_{(c_v^{(t)}, d_v^{(t)}) \in L_v^{(t)}} c_v^{(t)}$.

The node sequence of k_{uv}^* is obtained by backtracking the associated predecessor node $\pi_v^{(t)}$.

Output c_{uv}^* and the node sequence of the minimum-cost feasible subpath k_{uv}^* .

End for

Terminate the algorithm.

Else

Go to Step 1.

End if

Following Procedure 1, the minimum-cost feasible subpath k_{uv}^* and its cost c_{uv}^* are determined between any two charging station nodes (or an origin node and a destination node, or an origin/destination node and a charging station node). Subsequently, an examination of the node sequence along k_{uv}^* is conducted. If there is no additional charging station node along this subpath, except for its head node v and tail node u , it qualifies as a pure subpath. In such cases, add k_{uv}^* into H and A^M . Additionally, the set of

nodes within the metanetwork, denoted as N^M , includes all charging station nodes, origin nodes, and destination nodes. As a result, a station-subpath metanetwork concerning the driving range D is constructed.

3.1.2. A single-criterion label-setting algorithm in the second phase

Within the station-subpath metanetwork, the linear programming model defined in Eqs. (5)–(9) represents a simple optimal network flow problem, offering the opportunity to be solved through several well-established methods. One such method is the single-criterion label-setting algorithm, with detailed steps elucidated in Procedure 2.

Note that Procedure 2 determines travel costs incurred by travelers originating from a single node. For the computation of the total travel cost across the metanetwork, this procedure can be reiterated for each origin node r .

Procedure 2 A single-criterion label-setting algorithm

Step 0: Initialization.

Initialize the set of permanently labeled nodes to $S^P := \emptyset$ and the set of temporarily labeled nodes to $S^T := N^M$.

Initialize the predecessor node to $\pi_v := -1$ for each node $v \in N^M$.

Initialize the label to $l_r := 0$ for the origin node r and the label to $l_v := +\infty$ for each node $v \in N^M \setminus \{r\}$.

Step 1: Label update.

Let $u \in S^T$, where $l_u = \min_{v \in S^T} l_v$.

$S^P := S^P \cup \{u\}$.

$S^T := S^T \setminus \{u\}$.

For each link $(u, v) \in A^M$ do

 If $l_u + c_{uv} < l_v$ then

$l_v := l_u + c_{uv}$.

$\pi_v^{(1)} := u$.

 End if

End for

Step 2: Termination check.

If $|S^P| \neq |N^M|$ then

 Go to Step 1.

End if

Step 3: Network flow assignment.

For each destination node s do

l_s is the cost of the minimum-cost path from origin node r to destination node s .

 The node sequence of the minimum-cost path is obtained by backtracking π_s .

 Assign flows q_{rs} to the minimum-cost path.

End for

Calculate the total travel costs incurred by travelers originating from origin node r : $\sum_{(s:(r,s) \in W)} l_s q_{rs}$.

By employing Procedure 1 and Procedure 2, once the locations of charging stations are determined, the optimal network flow pattern and the optimal total travel cost within uncongested networks can be easily obtained.

3.2. A convex combinations method embedding a multi-criterion label-correcting procedure for deriving network flows in congested networks

Upon determining the charging station locations, the optimal charging station location problem in congested traffic networks collapses to a traffic assignment problem with relays (Xie and Jiang, 2016), as demonstrated in Eqs. (6) and (7), (13–21).

Therefore, this problem can be efficiently addressed by employing established algorithms commonly used for solving traffic assignment problems, such as the convex combinations method. However, it is important to note that in addressing the traffic assignment problem with relays through the convex combinations method, the underlying subproblem manifests as a network flow problem with relays (Xie and Jiang, 2016). In this scenario, travelers prioritize their minimum-cost feasible paths rather than their minimum-cost paths to finish their trips.

Further elaboration on the convex combinations method is available in Subsection 3.2.1. Additionally, Subsection 3.2.2 introduces a specifically devised multi-criterion label-correcting algorithm tailored to address the network flow problem with relays.

3.2.1. A convex combinations method

In the convex combinations method, we first formulate the subproblem as a mixed integer linear programming model outlined in Eqs. (6) and (7), (13–21), (24), with link costs determined by the network flow pattern \bar{x}_{ij} , $\forall (i, j) \in A$. We name the optimal solution of this model, x_{ij} , $\forall (i, j) \in A$, as the auxiliary flow pattern with respect to \bar{x}_{ij} , $\forall (i, j) \in A$.

$$\min \sum_{(i,j) \in A} x_{ij} c_{ij}(\bar{x}_{ij}) \quad (24)$$

subject to Eqs. (6)–(7), (13)–(21)

The algorithm begins by setting \bar{x}_{ij} to 0 for every link $(i, j) \in A$. It proceeds by solving the subproblem, resulting in the auxiliary flow pattern x_{ij} , $\forall (i, j) \in A$. Subsequently, combining x_{ij} with \bar{x}_{ij} generates an updated \bar{x}_{ij} , $\forall (i, j) \in A$. This process iterates, continually solving the subproblem and adjusting the traffic network flow pattern until the convergence criterion is met. Further details regarding the convex combinations method can be found in Procedure 3.

Procedure 3 A convex combinations method

Step 0: Initialization.

Perform an all-or-nothing assignment for all O-D pairs based on $c_{ij} = c_{ij}(0)$ for each link $(i, j) \in A$ using the multi-criterion label-correcting algorithm in Procedure 4. This leads to the initial flow $x^1 = \{x_{ij}^1\}$.

Set the iteration counter $t := 1$ and the parameter $\kappa := 10^{-4}$.

Step 1: Direction.

Update the travel cost $c_{ij} := c_{ij}(x_{ij}^t)$ for each link $(i, j) \in A$.

Perform an all-or-nothing assignment for all O-D pairs based on c_{ij} for each link $(i, j) \in A$ using the multi-criterion label-correcting algorithm in Procedure 4. This results in the auxiliary flow $y^t = \{y_{ij}^t\}$.

Step 2: Step size.

Find γ_t that is the optimal solution of the following one-variable convex programming model:

$$\begin{aligned} \min \sum_{(i,j)} \int_0^{x_{ij}^t + \gamma(y_{ij}^t - x_{ij}^t)} c_{ij}(\tau) d\tau \\ \text{s.t. } 0 \leq \gamma \leq 1 \end{aligned}$$

Update the traffic flow $x_{ij}^{t+1} := x_{ij}^t + \gamma_t(y_{ij}^t - x_{ij}^t)$ for each link $(i, j) \in A$.

Step 3: Optimality check.

If the convergence criterion, $\frac{\sqrt{\sum_{(i,j)} (x_{ij}^{t+1} - x_{ij}^t)^2}}{\sum_{(i,j)} x_{ij}^t} \leq \kappa$, is met then

Output the current solution $x^{t+1} = \{x_{ij}^{t+1}\}$ regarded as the optimal solution.

Terminate the algorithm.

Else

$t := t + 1$.

Go to Step 1.

End if

It is important to note that Procedure 3 can also be utilized to determine the network flow pattern following the system optimum principle in congested networks. This adaptation requires two adjustments:

- (1) In the first line of Step 1, modifying “update travel cost $c_{ij} := c_{ij}(x_{ij}^t)$ for each link $(i, j) \in A$ ” to “update travel cost $c_{ij} := c_{ij}(x_{ij}^t) + \frac{\partial c_{ij}(x_{ij})}{\partial x_{ij}} x_{ij}^t$ for each link $(i, j) \in A$ ”;
- (2) In Step 2, changing “ $\min \sum_{(i,j)} \int_0^{x_{ij}^t + \gamma(y_{ij}^t - x_{ij}^t)} c_{ij}(\tau) d\tau$ ” to “ $\min \sum_{(i,j)} [x_{ij}^t + \gamma(y_{ij}^t - x_{ij}^t)] c_{ij}(x_{ij}^t + \gamma(y_{ij}^t - x_{ij}^t))$ ”, where $c_{ij}(x_{ij}^t + \gamma(y_{ij}^t - x_{ij}^t))$ indicates the cost of link (i, j) when the traffic flow rate on this link is $x_{ij}^t + \gamma(y_{ij}^t - x_{ij}^t)$.

3.2.2. A multi-criterion label-correcting algorithm

Based on the definition of the feasible path, for each node j , we introduce a label that encompasses three attributes: c_j , d_j , and \bar{d}_j , which represent the travel cost from the origin node, the driving distance from the last charging station (or from the origin if not passing any charging station), and the critical driving range from the origin node. Consequently, a label of a node j can be represented as $l_j = (c_j, d_j, \bar{d}_j)$.

The algorithm starts by initializing L_j , the set of Pareto-optimal labels for each node j , to $\{(c_{rj}, d_{rj}, d_{rj})\}$, where c_{rj} and d_{rj} represent the cost and physical length of the link connecting nodes r and j , respectively. If r and j are not connected in the traffic network, both values are set to infinity; if j is the origin node r , both values are set to zero. Subsequently, for every link (i, j) in the traffic network and every label $l_i = (c_i, d_i, \bar{d}_i)$ in the set of Pareto-optimal labels of node i , generate a new label $(c_i + c_{ij}, d_i + d_{ij}, \max\{d_i + d_{ij}, \bar{d}_i\})$ and add it to the set of Pareto-optimal labels of node j . Then perform a Pareto-optimal dominance check on this label set with respect to these three attributes, i.e., delete those labels that are dominated by other labels with respect to these three attributes. After that, verify whether each label is feasible, i.e., delete $l_j = (c_j, d_j, \bar{d}_j)$ from the Pareto-optimal label set L_j of node j if $\bar{d}_j > D$. The iteration would not stop until either the set of Pareto-optimal labels of any node remains unchanged or this process has been conducted for $|N| - 1$ times, where $|N|$ represents the number of nodes in the traffic network. Finally, for each node j , the label with the minimum value of c_j represents the minimum-cost feasible path from the origin node r to node j . The sequence of nodes along this path can be obtained by backtracking through their associated predecessor nodes.

For a comprehensive understanding of this multi-criterion label-correcting algorithm, please refer to Procedure 4. Note that Procedure 4 is specifically designed to determine the network flows for travel demands originating from a single origin node. To capture the network flows for all travel demands, the procedure needs to be iterated for each origin node r within the network.

Procedure 4 A multi-criterion label-correcting algorithm

Step 0: Initialization.

Initialize the iteration counter to $t := 0$.

For each node $j \in N$ do

Initialize the set of predecessor nodes to $\Pi_j^{(t)} := \{\pi_j^{(t)}\} := \{r\}$ and the set of labels to $L_j^{(t)} := \emptyset$.

If $j = u$ then

$L_j^{(t)} := L_j^{(t)} \cup \{l_j^{(t)}\}$, where $l_j^{(t)} = (0, 0, 0)$.

Else if nodes u and j are connected then

$L_j^{(t)} := L_j^{(t)} \cup \{l_j^{(t)}\}$, where $l_j^{(t)} = (c_{uj}, d_{uj}, d_{uj})$, c_{uj} and d_{uj} are respectively the cost and distance of the link connecting these two nodes.

(continued on next page)

```

Else
   $L_j^{(t)} := L_j^{(t)} \setminus \{l_j^{(t)}\}$ , where  $l_j^{(t)} = (+\infty, +\infty, +\infty)$ .
End if
End for
Step 1: Label update.
 $t := t + 1$ .
 $L_j^{(t)} := L_j^{(t-1)}$ ,  $\Pi_j^{(t)} := \Pi_j^{(t-1)}$ .
For each link  $(i, j) \in A$  do
  If node  $i$  is a charging station node then
     $\bar{d}_i^{(t-1)} := \max\{d_i^{(t-1)}, d_i^{(t-1)}\}$  for each label  $l_i^{(t-1)} \in L_i^{(t-1)}$ .
     $d_i^{(t-1)} := 0$  for each label  $l_i^{(t-1)} \in L_i^{(t-1)}$ .
  End if
  For each  $l_j^{(t-1)} \in L_j^{(t-1)}$  do
     $(c_j^{(t)}, d_j^{(t)}, \bar{d}_j^{(t)}) := (c_j^{(t-1)} + c_{ij}, d_j^{(t-1)} + d_{ij}, \max\{d_j^{(t-1)} + d_{ij}, \bar{d}_j^{(t-1)}\})$ .
    If  $(c_j^{(t)}, d_j^{(t)}, \bar{d}_j^{(t)})$  is not dominated by any  $l_j^{(t-1)}$  in  $L_j^{(t-1)}$  then
       $L_j^{(t)} := L_j^{(t)} \cup \{(c_j^{(t)}, d_j^{(t)}, \bar{d}_j^{(t)})\}$ ,  $\Pi_j^{(t)} := \Pi_j^{(t)} \cup \{i\}$ .
      If any  $l_j^{(t)}$  in  $L_j^{(t)}$  is dominated by  $(c_j^{(t)}, d_j^{(t)}, \bar{d}_j^{(t)})$  then
         $L_j^{(t)} := L_j^{(t)} \setminus \{l_j^{(t)}\}$ ,  $\Pi_j^{(t)} := \Pi_j^{(t)} \setminus \{i\}$ .
      End if
    End if
  End for
  If  $\bar{d}_j^{(t)} > D$ ,  $\forall l_j^{(t)} \in L_j^{(t)}$  then
     $L_j^{(t)} := L_j^{(t)} \setminus \{l_j^{(t)}\}$ ,  $\Pi_j^{(t)} := \Pi_j^{(t)} \setminus \{\pi_j^{(t)}\}$ .
  End if
End for
Step 2: Termination check.
If  $t = |N| - 1$  or  $L_j^{(t)} = L_j^{(t-1)}$  for any  $j \in N$  then
  For each destination node  $s$  do
    The cost of the minimum-cost feasible path from  $r$  to  $s$  is  $c_s^* = \min_{(c_i^{(t)}, d_i^{(t)}, \bar{d}_i^{(t)}) \in L_i^{(t)}} c_i^{(t)}$ .
    The node sequence along the minimum-cost feasible path can be obtained by backtracking the associated predecessor node  $\pi_s^{(t)}$ .
    Assign flows  $q_{rs}$  to the minimum-cost feasible path.
  End for
  Terminate the algorithm.
Else
  Go to Step 1.
End if

```

Following Procedure 3 and Procedure 4, once determining the locations of charging stations, the network flow pattern following either the user equilibrium principle or the system optimum principle and the associated total travel cost within congested networks can be effectively solved.

3.3. A branch-and-bound algorithm for determining optimal locations in uncongested and congested networks

In this part, we introduce the classic branch-and-bound algorithm to solve the optimal location problems for both uncongested and congested network cases. For simplicity, we use $z_l = 1$ to signify the construction of a charging station at candidate node l , $z_l = 0$ when no charging station is erected at node l , and $z_l = -1$ when the decision regarding a charging station at candidate node l is pending. The task is to determine the optimal charging station locations $z = [z_1, z_2, \dots, z_l, \dots, z_{|L|}]$ and simultaneously ensure the total investment cost of the solution z , $\sum_{\{l|z_l=1\}} e_l z_l$, does not surpass the budget limit G , where e_l signifies the cost of building a charging station at node l .

Subsequently, a branch-and-bound tree is constructed with a depth of $|L| + 1$ to represent the decisions pertaining to charging station locations. Each layer, denoted as l , corresponds to the decision-making process for z_l . Additionally, we employ a superscript p to distinguish different vertices within the same layer l of the branch-and-bound tree, the value of which ranges from 1 to 2^l and depends on the values of the first l variables in z_l . Specifically, $p = 1 + \sum_{i=1}^l (2^{l-i} z_i)$, $\forall l \geq 1$. For instance, $z_1^1 = [0, -1, \dots, -1]$, $z_1^2 = [1, -1, \dots, -1]$.

The branching rule is as follows: for each vertex except for leaf vertices, denoted as $z_{l-1}^p = [z_1 \neq -1, z_2 \neq -1, \dots, z_{l-1} \neq -1, z_l = -1, z_{l+1} = -1, \dots, z_{|L|} = -1]$, $l - 1 \neq |L|$, we can branch it into a left subtree vertex $z_l^{2p-1} = [z_1 \neq -1, z_2 \neq -1, \dots, z_{l-1} \neq -1, z_l = 0, z_{l+1} = -1, \dots, z_{|L|} = -1]$ and a right subtree vertex $z_l^{2p} = [z_1 \neq -1, z_2 \neq -1, \dots, z_{l-1} \neq -1, z_l = 1, z_{l+1} = -1, \dots, z_{|L|} = -1]$. Here, the values of z_1, z_2, \dots, z_{l-1} in both z_l^{2p-1} and z_l^{2p} are the same as the values of z_1, z_2, \dots, z_{l-1} in z_{l-1}^p , respectively.

Moreover, since Procedures 1 to 4 require a predetermined distribution solution of charging station locations, the use of z_l with decimal values is inappropriate. Therefore, employing the commonly used linear relaxation method becomes unsuitable for determining the lower bound for a vertex z_l^p in the branch-and-bound tree.

Nevertheless, Proposition 2 presents an alternative method that enables the derivation of the lower bound for the vertex z_l^p in uncongested networks. Specifically, this method involves transforming $z_\theta = -1$ to $z_\theta = 1$ for all $\theta = l + 1, l + 2, \dots, |L|$ in the vertex

z_l^p , resulting in a new solution \bar{z}_l^p . The total travel cost obtained from the solution \bar{z}_l^p using Procedure 1 and Procedure 2 can serve as the lower bound for the vertex z_l^p .

On the other hand, in congested networks where charging station locations are determined as z_l^p , the total travel cost over the network when travelers follow the system optimum principle is less than that when travelers follow the user equilibrium principle, i.e., $C_{SO}(z_l^p) < C_{UE}(z_l^p)$. This well-known conclusion, combined with Proposition 3 that $C_{SO}(\bar{z}_l^p) \leq C_{SO}(z_l^p)$, provides an alternative method to derive the lower bound for the vertex z_l^p in congested networks. Specifically, transforming $z_\theta = -1$ to $z_\theta = 1$ for all $\theta = l+1, l+2, \dots, |L|$ in the vertex z_l^p generates a new solution \bar{z}_l^p . The total travel cost incurred by travelers following the system optimum principle with the solution \bar{z}_l^p , denoted as $C_{SO}(\bar{z}_l^p)$, can serve as the lower bound for the vertex z_l^p .

Following the depth-first-search rule and the “root vertex - right subtree vertex - left subtree vertex” order of examining vertices, this algorithm begins by initializing U , the stack containing unexamined vertices, to $\{z_0\}$, where z_0 is the root vertex of this branch-and-bound tree. In z_0 , all values of z_l are set to -1 , indicating an undecided status regarding the construction of charging stations at node l . The algorithm terminates when all vertices in the branch-and-bound tree have been examined or pruned, i.e., when the stack is empty.

Additional details on the branch-and-bound algorithm can be found in Procedure 5, where $C(z)$ represents the total travel cost over uncongested networks with a determined solution of charging station locations z . Moreover, $C_{UE}(z)$ and $C_{SO}(z)$ represent the total travel costs incurred by travelers following the user equilibrium principle and the system optimum principle in congested networks with a determined solution of charging station locations z , respectively.

Procedure 5 A branch-and-bound algorithm

Step 0: Initialization.

Initialize the stack containing unexamined vertices to $U := \{z_0\}$, where $z_0 = [-1, -1, \dots, -1, -1]$.

Initialize the incumbent optimal solution to $z_{\min} := [0, 0, \dots, 0]$.

Calculate the incumbent optimal value: $\begin{cases} C_{\min} := C(z_{\min}) & \text{in uncongested networks} \\ C_{\min} := C_{UE}(z_{\min}) & \text{in congested networks} \end{cases}$.

Step 1: Search.

If U is not empty then

 Peek the top element on stack U and name it $z = [z_1, z_2, \dots, z_l, \dots, z_{|L|}]$.

 If $\sum_{\{l|z_l=1\}} e_l z_l \leq G$ then

 Calculate the lower bound value for z : $\begin{cases} C(\bar{z}) & \text{in uncongested networks} \\ C_{SO}(\bar{z}) & \text{in congested networks} \end{cases}$

 If the lower bound value is greater than or equal to C_{\min} then

 Go to Step 2.

 Else if $\exists z_l \in z$ such that $z_l = -1$ then

 Go to Step 3.

 Else

 Update the incumbent optimal solution: $z_{\min} := z$.

 Update the incumbent optimal value: $\begin{cases} C_{\min} := C(z) & \text{in uncongested networks} \\ C_{\min} := C_{UE}(z) & \text{in congested networks} \end{cases}$.

 Go to Step 2.

 End if

Else

 Go to Step 2.

End if

Else

 Go to Step 4.

End if

Step 2: Pruning.

Pop the top element z from stack U .

Go to Step 1.

Step 3: Branching.

Fetch a solution $z_{l-1}^p = [z_1, z_2, \dots, z_l, \dots, z_{|L|}]$, where the values of z_1, z_2, \dots , and z_{l-1} equal 0 or 1, while the values of $z_l, z_{l+1}, \dots, z_{|L|}$ equal -1 .

Branch z_{l-1}^p into two vertices: $z_l^{2p-1} = [z_1, \dots, z_{l-1}, z_l = 0, \dots, z_{|L|}]$ and $z_l^{2p} = [z_1, \dots, z_{l-1}, z_l = 1, \dots, z_{|L|}]$, where the values of z_θ in z_l^{2p-1}, z_l^{2p} , and z_l are the same, $\forall \theta = 1, 2, \dots, l-1, l+1, \dots, |L|$.

Pop the top element z_{l-1}^p from stack U .

Push z_l^{2p-1} onto stack U .

If $l = |L|$ then

 Push z_l^{2p} onto stack U .

 Go to Step 1.

Else

 Let z_l^{2p} be the updated vertex that would be branched.

$l := l + 1$.

 Go to Step 3.

End if

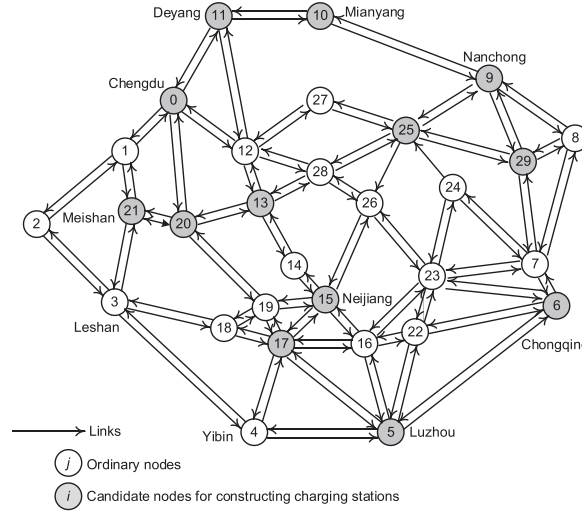
Step 4: Termination.

Output C_{\min} and z_{\min} .

Table 7

Comparison between the algorithmic procedures for uncongested and congested networks.

	Uncongested networks	Congested networks
Algorithm for finding optimal charging station locations	Procedure 5;	Procedure 5;
Algorithm for finding network flows	First phase: Procedure 1; Second phase: Procedure 2;	Procedure 3 embedding Procedure 4;

**Fig. 3.** Sichuan Basin highway network.

3.4. A comparison between the algorithmic procedures for uncongested and congested networks

A comparative summary of the algorithms used for optimal charging station location problems both with and without incorporating traffic congestion is presented in Table 7.

The differences between the procedural steps for deploying the Procedure 5 in the uncongested network versus the congested network are primarily centered around the evaluation method of a solution and the subregion bounding strategy:

- (1) In uncongested networks, given a vertex z where all charging station construction decisions are determined, the evaluation of the vertex z relies on the total travel cost over the network denoted by $C(z)$. This cost is derived from Procedure 1 and Procedure 2. Conversely, in congested networks, the evaluation of the vertex z is based on the total travel cost over the network when travelers adhere to the user equilibrium principle $C_{UE}(z)$, which is derived from Procedure 3 and Procedure 4.
- (2) Altering $z_i = -1$ to $z_i = 1$ in a given vertex z can result in a new vertex \bar{z} . In uncongested networks, the total travel cost derived from the new vertex \bar{z} using Procedure 1 and Procedure 2, denoted as $C(\bar{z})$, serves as the lower bound for the original vertex z . Conversely, in congested networks, the total travel cost incurred by travelers following the system optimum principle with the new vertex \bar{z} using Procedure 3 and Procedure 4, denoted as $C_{SO}(\bar{z})$, acts as the lower bound for the original vertex z .

4. Numerical analysis

4.1. Example networks

Fig. 3 illustrates the topology of the Sichuan Basin highway network, which consists of 30 nodes (13 of which are candidate nodes for charging stations), 116 links, and an extensive set of 90 O-D pairs. For the travel demand table of the Sichuan Basin highway network, please refer to Zeng et al. (2024).

Table 8 provides detailed link information for the Sichuan Basin highway network, where $i, j, c_{0,ij}/c_{ij}$ (unit: hour), d_{ij} (unit: kilometer), v_{ij} (unit: flow rate) denote the tail node of the link, the head node of the link, the free-flow travel cost of the link in congested networks or the travel cost of the link in uncongested networks, the physical length of the link in traffic networks, and the capacity of the link in congested networks, respectively. Note that the attributes of link (i, j) are the same as those of link (j, i) in the Sichuan Basin highway network. Therefore, we only present the information of 58 links in Table 8.

Without loss of generality, assuming the construction cost of each charging station at any node equivalent (i.e., e_l is fixed across all candidate nodes l for constructing charging stations) can simplify our analysis. In such a condition, the maximum number of charging stations that can be built is equal to the construction budget limit.

Table 8

Link information of the Sichuan Basin highway network.

	$c_{0,ij}/c_{ij}$	d_{ij}	v_{ij}	(i, j)	$c_{0,ij}/c_{ij}$	d_{ij}	v_{ij}	(i, j)	$c_{0,ij}/c_{ij}$	d_{ij}	v_{ij}
(0, 1)	0.8	80	5000	(7, 23)	1.6	168	1000	(15, 19)	1.0	108	1000
(0, 11)	1.8	170	6000	(7, 24)	2.0	198	1000	(15, 26)	1.6	166	1000
(0, 12)	1.2	124	5000	(7, 29)	1.6	162	1000	(16, 17)	1.4	142	1000
(0, 20)	1.6	156	1000	(8, 9)	1.8	170	1000	(16, 22)	0.8	78	1000
(1, 2)	2.2	218	1000	(8, 29)	0.6	76	1000	(16, 23)	1.4	142	1000
(1, 21)	0.8	96	5000	(9, 10)	3.4	334	1000	(17, 18)	1.0	106	1000
(2, 3)	2.2	228	1000	(9, 25)	1.4	150	1000	(17, 19)	0.8	86	1000
(3, 4)	3.4	314	1000	(9, 29)	1.2	128	1000	(18, 19)	0.8	70	1000
(3, 18)	1.4	154	1000	(10, 11)	1.2	122	5000	(19, 20)	2.0	190	1000
(3, 21)	1.4	144	2000	(11, 12)	2.2	216	1000	(20, 21)	1.0	106	1000
(4, 5)	2.8	236	1000	(12, 13)	0.8	88	2000	(22, 23)	1.2	126	1000
(4, 17)	1.6	152	1000	(12, 27)	2.0	202	1000	(23, 24)	1.4	136	1000
(5, 6)	3.6	368	1000	(12, 28)	1.2	124	1000	(23, 26)	1.8	176	1000
(5, 16)	1.2	124	1000	(13, 14)	1.2	120	2000	(24, 25)	1.0	106	1000
(5, 17)	2.0	198	1000	(13, 20)	1.2	128	1000	(25, 26)	1.4	134	1000
(5, 22)	1.6	154	1000	(13, 28)	1.0	112	1000	(25, 27)	0.8	82	1000
(6, 7)	0.8	80	2000	(14, 15)	0.8	74	2000	(25, 28)	1.6	152	1000
(6, 22)	2.2	218	1000	(15, 16)	1.0	90	2000	(25, 29)	1.8	174	1000
(6, 23)	1.8	188	1000	(15, 17)	0.8	90	1000	(26, 28)	1.0	94	1000
(7, 8)	2.2	222	1000								

4.2. Network flow patterns

This subsection examines variations in link flow patterns across diverse construction budget limits and driving ranges within both uncongested and congested Sichuan Basin highway networks. With the driving ranges of 300 km and 500 km and construction budget limits of 6 and 10, this yields four distinct scenarios. The network flow patterns for these scenarios within the uncongested and congested networks are respectively illustrated in Figs. 4 and 5. Considering results indicate that flow rates on link (i, j) coincide with those on link (j, i) across all scenarios, we exclusively present the flow patterns for the 58 detailed links, as outlined in Table 8.

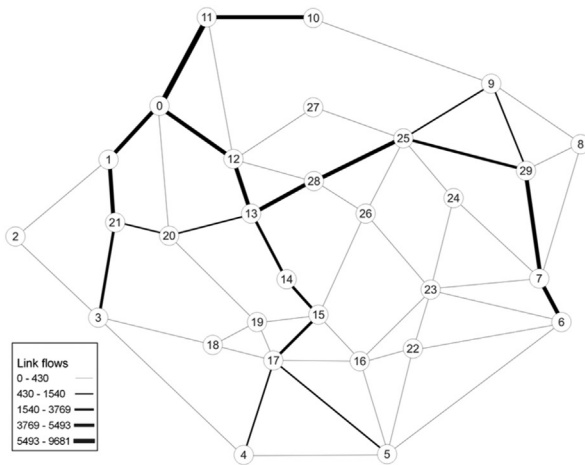
Firstly, it is evident that with a driving range of 300 km, travelers traversing between Luzhou (Node 5) and Chongqing (Node 6) within both uncongested and congested Sichuan Basin highway networks are compelled to complete their journeys via paths such as Path 5-16-15-26-25-29-7-6 (as depicted in Fig. 5(a) and (b)), Path 5-17-15-14-13-28-25-29-7-6 (as shown in Fig. 4(a)), or Path 5-16-15-14-13-28-25-29-7-6 (as illustrated in Fig. 4(b)). These paths entail significantly higher costs compared to the minimum-cost path, 5-6. This discrepancy arises due to the driving range of 300 km, which fails to cover Link 5-6 spanning 378 km. In such a situation, considerable inconvenience is encountered. This underscores the critical role of EV driving ranges in completing intercity trips, particularly when the minimum-cost path passes by fewer interchanges or cities.

Moreover, when incorporating traffic congestion into consideration while adhering to the constant driving range and budget limit, there is an increase in the number of utilized links within the traffic network. Specifically, the numbers of used links within the uncongested Sichuan Basin highway networks in the four scenarios are respectively 52, 60, 84, and 84, while the numbers of used links within the congested Sichuan Basin highway networks in the four scenarios are 58, 68, 96, and 96, respectively. This phenomenon stems from the fact that, in the presence of traffic congestion, both link costs and path costs become flow-dependent. Consequently, for each O-D pair, there may be several minimum-cost feasible paths utilized. Along these newly utilized paths, there may be some previously unutilized links. As a result, the overall number of utilized links within the traffic network experiences an escalation. For instance, travelers traveling between Luzhou (Node 5) and Nanchong (Node 9) may opt not to traverse Path 5-16-15-26-25-9 as depicted in Fig. 4(a), whereas they choose to do so in Fig. 5(a). Consequently, links such as 5-16, 16-15, 15-26, and 26-25, which remain unused in Fig. 4(a), become utilized in Fig. 5(a).

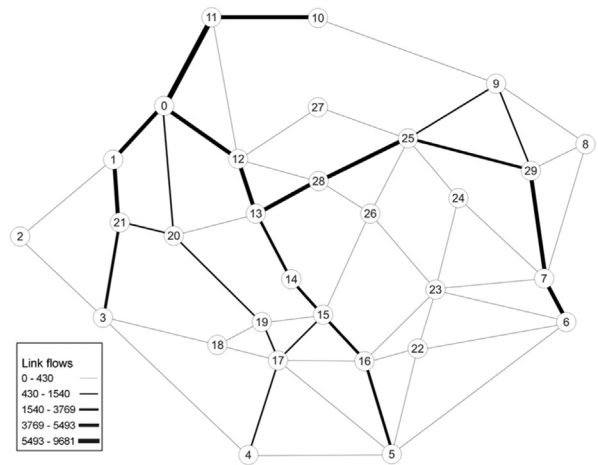
4.3. Travel costs

This subsection uses the Sichuan Basin highway network as an example to explore variations in total travel costs among travelers across diverse construction budget limits and driving ranges in both uncongested and congested networks. The driving range varies incrementally from 300 km to 500 km in steps of 50 km, and the construction budget limit is set at 6, 8, and 10. Consequently, this results in 30 scenarios (i.e., 5 driving ranges \times 3 budget limits \times 2 networks, without and with incorporating traffic congestion), as demonstrated in Tables 9 and 10.

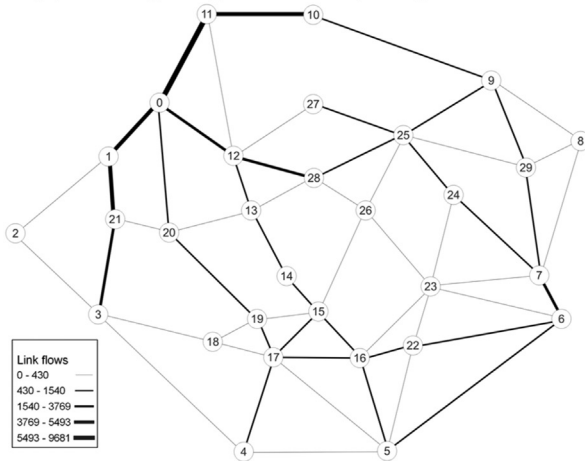
In Table 9, it is observed that as the driving range increases while the budget limit is determined, the total cost consistently decreases. This trend suggests that a higher driving range correlates with a lower total travel cost in uncongested networks, aligning with Proposition 4. However, Table 10 shows a different scenario where increasing the driving range does not invariably result in decreased or equal total travel costs. For instance, when the budget limit is set at 6, 8, or 10, an increase in the driving range from 450 km to 500 km leads to a rise in total travel costs, supporting the insights outlined in Remark 1.



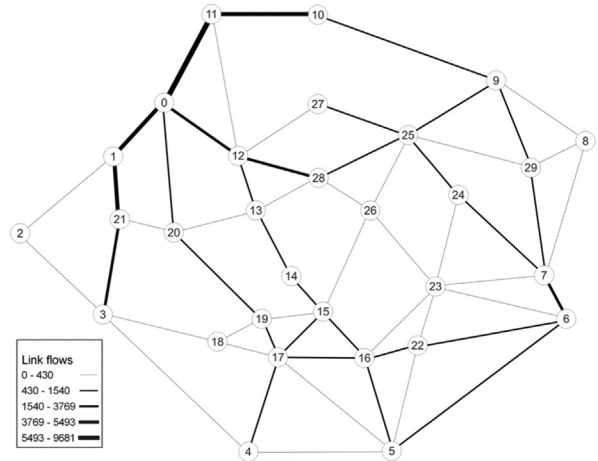
(a) Driving range = 300 km, budget limit = 6



(b) Driving range = 300 km, budget limit = 10



(c) Driving range = 500 km, budget limit = 6



(d) Driving range = 500 km, budget limit = 10

Fig. 4. Network flow patterns in the uncongested Sichuan Basin highway network.

Table 9

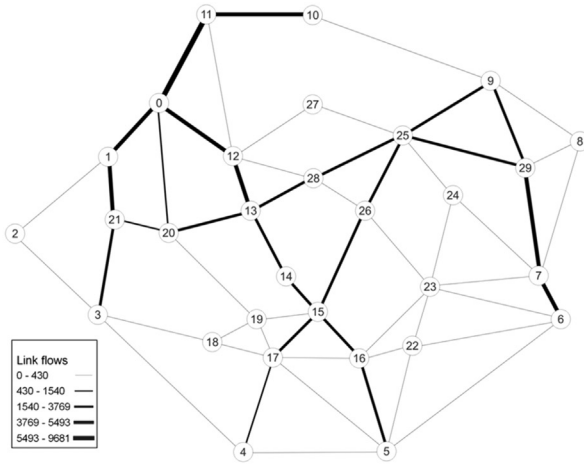
Total travel cost variations of the uncongested Sichuan Basin highway network.

	Budget limit = 6	Budget limit = 8	Budget limit = 10
Driving range = 300 km	196,010	193,679	193,679
Driving range = 350 km	181,881	180,486	179,615
Driving range = 400 km	164,253	163,302	163,110
Driving range = 450 km	161,513	161,390	161,390
Driving range = 500 km	161,290	161,290	161,290

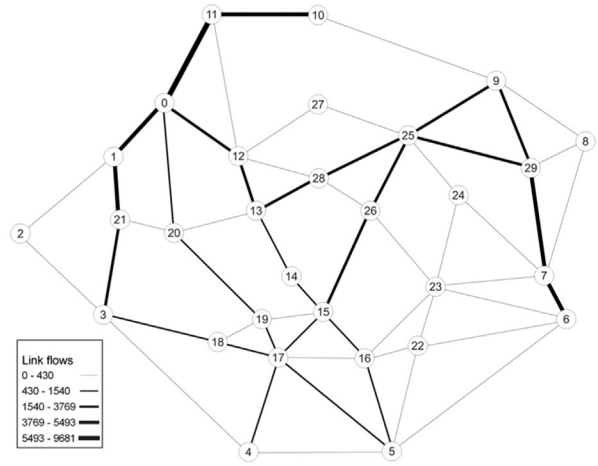
Table 10

Total travel cost variations of the congested Sichuan Basin highway network.

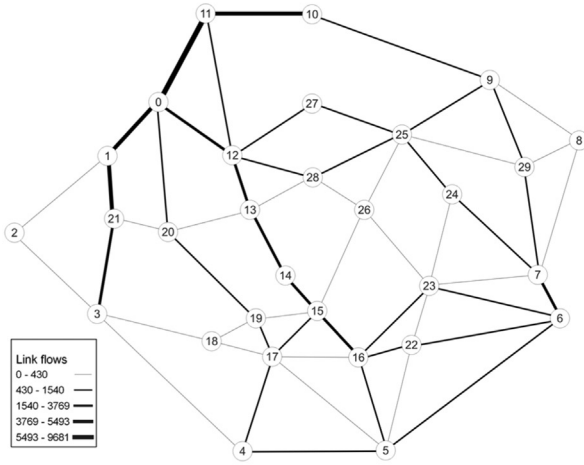
	Budget limit = 6	Budget limit = 8	Budget limit = 10
Driving range = 300 km	1,391,450	1,352,260	1,352,250
Driving range = 350 km	1,150,970	1,124,820	1,117,710
Driving range = 400 km	211,414	204,502	203,448
Driving range = 450 km	195,108	194,422	194,422
Driving range = 500 km	198,300	198,300	195,170



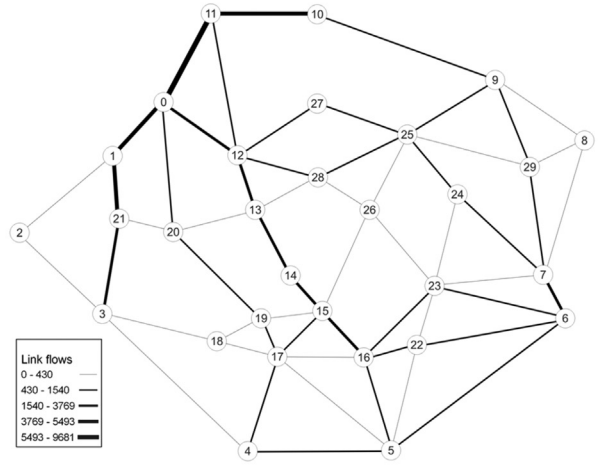
(a) Driving range = 300 km, budget limit = 6



(b) Driving range = 300 km, budget limit = 10



(c) Driving range = 500 km, budget limit = 6



(d) Driving range = 500 km, budget limit = 10

Fig. 5. Network flow patterns in the congested Sichuan Basin highway network.

Moreover, across both [Tables 9 and 10](#), regardless of the driving range, an increase in the budget limit consistently leads to a decreased or unchanged total travel cost. This observation aligns with the assertions in Proposition 3. Notably, the reduction is more pronounced when the driving range is lower in both tables.

4.4. Optimal solutions and computational performances

This subsection aims to compare the optimal charging station locations and the computing time required for obtaining optimal solutions in scenarios with and without incorporating traffic congestion, considering various budget limits and driving ranges. Comparing the computing time results of two distinct solution frameworks for different problems does not inherently determine the performance superiority of one algorithm over another. Rather, this comparison is presented to provide insights into how the incorporation of traffic congestion influences the complexity of the problem. The algorithms were coded in C++ and performed on a computer equipped with an Intel Core i7-11390H CPU and 16 GB RAM. Using the Sichuan Basin highway network as an example, the construction budget limits of 6, 8, and 10, along with driving ranges of 300 km, 350 km, 400 km, 450 km, and 500 km were considered. The optimal charging station locations and the computing time results for congested and uncongested networks are depicted in [Table 11 and 12](#) respectively.

In the uncongested Sichuan Basin highway network, the number of charging stations established in the optimal scheme of charging station locations always equals the budget limit. On one hand, this is because, in the branch-and-bound algorithm designed in this paper, the depth-first-search rule and the root vertex-right subtree vertex-left subtree vertex order of examining vertices are followed, prioritizing the examination of solutions with a higher number of built charging stations. On the other hand, in uncongested networks, establishing a charging station at a node where none exists will reduce or keep the total travel cost unchanged. Hence, the optimal

Table 11

Optimal solution and computing time variations of the uncongested Sichuan Basin highway networks.

Driving range (km)	Budget limit	Optimal charging station locations	Number of network evaluations	CPU time (s)	
				Single evaluation	Total
300	6	0, 13, 17, 21, 25, 29	664	0.0551	36.6
	8	0, 13, 15, 17, 20, 21, 25, 29	458	0.0587	26.9
	10	0, 5, 6, 13, 15, 17, 20, 21, 25, 29	133	0.0639	8.5
350	6	0, 9, 13, 15, 25, 29	651	0.0568	37.0
	8	0, 9, 10, 11, 13, 15, 25, 29	313	0.0655	20.5
	10	0, 9, 10, 11, 13, 15, 17, 20, 25, 29	92	0.0587	5.4
400	6	0, 9, 10, 13, 15, 25	283	0.0594	16.8
	8	0, 9, 10, 13, 15, 17, 20, 25	141	0.0539	7.6
	10	0, 5, 9, 10, 11, 13, 15, 17, 20, 25	37	0.0676	2.5
450	6	0, 9, 10, 13, 17, 25	226	0.0580	13.1
	8	0, 5, 9, 10, 13, 15, 17, 25	81	0.0667	5.4
	10	0, 5, 6, 9, 10, 11, 13, 15, 17, 25	18	0.0722	1.3
500	6	0, 9, 11, 15, 17, 25	325	0.0618	20.1
	8	0, 5, 6, 9, 11, 15, 17, 25	78	0.0692	5.4
	10	0, 5, 6, 9, 10, 11, 13, 15, 17, 25	18	0.0722	1.3
Average		-	235	0.0627	13.9

Table 12

Optimal solution and computing time variations in the congested Sichuan Basin highway networks.

Driving range (km)	Budget limit	Optimal charging station locations	Number of network evaluations	CPU time (s)	
				Single evaluation	Total
300	6	0, 13, 15, 21, 25, 29	798	36.3	28,958.9
	8	0, 13, 15, 17, 20, 21, 25, 29	554	38.5	21,351.6
	10	0, 5, 9, 13, 15, 17, 20, 21, 25, 29	371	40.0	14,839.0
350	6	10, 11, 13, 15, 25, 29	800	36.6	29,252.9
	8	9, 10, 11, 13, 15, 20, 25, 29	433	25.7	11,147.8
	10	5, 9, 10, 11, 13, 15, 17, 20, 25, 29	285	24.4	6950.4
400	6	5, 9, 13, 15, 17, 25	670	14.2	9513.0
	8	5, 9, 11, 13, 15, 17, 20, 25	417	10.4	4354.3
	10	5, 6, 9, 10, 11, 13, 15, 17, 20, 25	358	8.5	3049.8
450	6	9, 10, 13, 15, 17, 25	601	8.7	5213.8
	8	5, 6, 9, 10, 13, 15, 17, 25	397	6.5	2572.1
	10	5, 6, 9, 10, 13, 15, 17, 25	560	6.3	3550.8
500	6	5, 13, 15, 17, 25, 29	2547	6.1	15,509.2
	8	5, 6, 13, 15, 17, 25, 29	4324	7.4	31,802.8
	10	5, 6, 13, 15, 17, 25, 29	5495	8.7	47,654.9
Average		-	1241	18.6	15,714.8

solution obtained by the branch-and-bound algorithm in this paper is definitely the first optimal solution found during the search (when multiple optimal solutions exist). The number of built charging stations in this solution must be the maximum among all optimal solutions, which is equal to the budget limit. Nevertheless, in the congested Sichuan Basin highway network, the established charging stations in the optimal scheme for charging station locations may be fewer than the budget limit. For instance, in scenarios like a driving range of 500 km with a budget limit of 8 or 10, the number of constructed charging stations only reaches 7. This discrepancy arises due to the likelihood that setting up a charging station at a node without one could potentially elevate the total travel cost in congested networks. Hence, more charging stations do not necessarily imply better outcomes.

Additionally, it is evident that an increase in the budget limit (while keeping the driving range constant) leads to a reduced computing time result for the optimal solution in the uncongested Sichuan Basin highway network. This effect stems from Proposition 3 that an increase in the budget limit results in a reduced total travel cost associated with the optimal solution or maintains it at the same value. In other words, the upper bound of the optimal value in the branch-and-bound algorithm decreases (or remains unchanged). Consequently, the likelihood of the lower bound value for a vertex being smaller than the upper bound of the optimal value rises. As a result, pruning operations become more probable, thereby decreasing the number of network evaluations and accelerating the convergence of the branch-and-bound algorithm. However, in the congested Sichuan Basin highway network, this conclusion does not always hold true (for instance, with a driving range of 500 km, when the budget limit increases from 6 to 8, the total computing time for the optimal solution also increases from 15,509.2 seconds to 31,802.8 seconds). For one thing, this occurs because, in congested networks, the total travel cost used to evaluate a scheme of charging station locations is based on the fact that travelers follow the user equilibrium principle, while computing the lower bound for a vertex involves considering the total travel cost based on the fact that travelers adhere to the system optimum principle. The probability of the latter being greater than the former is relatively low, resulting in a lower probability of pruning operations occurring. For another, a higher budget limit implies that the branch-and-bound algorithm initially examines vertices with a greater number of established charging stations, which in congested

networks might increase the total travel cost. This scenario might offer a higher incumbent optimal value (i.e., the upper bound of the optimal value) in the early stages of the branch-and-bound algorithm, potentially making pruning operations more difficult to occur. Therefore, this might lead to a greater number of network evaluations and a slower convergence speed of the branch-and-bound algorithm.

Furthermore, in the congested Sichuan Basin highway network, the total computing time for the optimal solution is approximately 1,100 times greater than that in the uncongested Sichuan Basin highway network, because the former involves both a greater number of network evaluations (the effect of this is relatively minor) and a greater average computing time per network evaluation (the effect of this is relatively greater). This stark contrast underscores how the incorporation of traffic congestion significantly exacerbates the computational complexity inherent in solving the charging station location problem.

5. Conclusions

This paper addresses and compares how to model and solve the optimal en-route charging station location problems for uncongested and congested highway networks, in analytical, numerical and computational ways. For uncongested networks, a metanetwork-based two-stage model is introduced, which involves multiple integer programming models minimizing the station-to-station subpath costs in the first stage and a mixed integer linear programming model minimizing the total travel cost in the second stage. For congested networks, a network-based bi-level model is proposed, the upper level of which is a mixed integer nonlinear programming model minimizing the total travel cost, and the lower level is also a mixed integer nonlinear programming model but addressing a traffic assignment problem with relays. Both models are addressed using the classic branch-and-bound algorithm, albeit employing distinct problem decomposition schemes, subregion bounding strategies, and network flow evaluation methods. In the context of uncongested networks, a two-phase approach is adopted: Initially, a bi-criterion label-correcting algorithm is utilized to construct a metanetwork, followed by the application of the branch-and-bound algorithm on this metanetwork. This process incorporates a single-criterion label-setting algorithm to determine network flows. Conversely, for congested networks, the branch-and-bound algorithm is directly applied to the original network, where a convex combinations method is employed to derive network flows.

An extensive mathematical analysis has been conducted, yielding several key managerial insights. Firstly, within uncongested networks, adding an extra charging station at a node lacking one in an existing solution of charging station locations results in a new solution that either lowers the total travel cost or keeps the total travel cost unchanged. However, this outcome does not occur in congested networks unless the network flow pattern follows the system optimum principle rather than the user equilibrium principle. Secondly, an increase in the budget limit can lead to a reduced or at least unchanged total travel cost in both uncongested and congested networks. Thirdly, expanding the driving range can decrease the total travel cost or keep the total travel cost unchanged in uncongested networks, but this does not apply to congested networks.

On the other hand, the observations gleaned from the numerical analysis in this paper are multifaceted. Firstly, it is observed that when the driving range and budget limit remain unchanged, incorporating traffic congestion into the problem leads to more links utilized in the traffic network. Secondly, an increase in the budget limit results in a reduced or equal total travel cost in both the uncongested and congested Sichuan Basin highway networks. Thirdly, while an increase in the driving range consistently decreases the total travel cost in the uncongested Sichuan Basin highway network, this relationship does not apply to the congested Sichuan Basin highway network. Finally, within the uncongested Sichuan Basin highway network, the number of selected charging stations in the optimal scheme of charging station locations always equals the budget limit. However, such phenomena are absent in the congested Sichuan Basin highway network. Additionally, the total computing time for the charging station location problem in the congested Sichuan Basin highway network is approximately 1,100 times higher than that in the uncongested Sichuan Basin highway network, indicating the incorporation of traffic congestion significantly amplifies the computational complexity of the en-route charging station location problem.

In conclusion, while this research has made significant strides in understanding the implications of traffic congestion on the formulation and solution of the en-route charging station location problem, several avenues for future research and potential limitations warrant consideration. Future studies could enhance realism and complexity by incorporating factors such as individual waiting times and charging costs, heterogeneous driving ranges of electric vehicles, capacity constraints of charging stations, different levels of traffic congestion, and diverse charging behaviors of EV drivers. Addressing these aspects could lead to more sophisticated models and solutions, thereby advancing the development of charging station location selection tools and accelerating the adoption and utilization of electric vehicles.

Declaration of competing interest

This paper we submitted to *Multimodal Transportation* is the original unpublished work by Xueqi Zeng and Chi Xie.

The manuscript or any variation of the paper has not been submitted to another publication previously. It does not contain any impermissible or confidential information or data from any source.

CRediT authorship contribution statement

Xueqi Zeng: Data curation, Formal analysis, Investigation, Validation, Visualization, Writing – original draft. **Chi Xie:** Conceptualization, Data curation, Funding acquisition, Methodology, Project administration, Resources, Supervision, Writing – review & editing.

Acknowledgments

This research is sponsored by the National Natural Science Foundation of China (Grant No. 72171175, 71890970, 72111540273) and Natural Science Foundation of Hainan Province (Grant No. 722MS046). The authors sincerely thank Dr. Zhaoyao Bao from Shanghai Jiao Tong University and Dr. Jiawei Li from Tongji University for sharing their computer code and providing technical support for this research.

References

- Arsilan, O., Karaşan, O.E., Mahjoub, A.R., Yaman, H., 2019. A branch-and-cut algorithm for the alternative fuel refueling station location problem with routing. *Transport. Sci.* 53, 1107–1125. doi:10.1287/trsc.2018.0869.
- Bao, Z., Xie, C., 2021. Optimal station locations for en-route charging of electric vehicles in congested intercity networks: a new problem formulation and exact and approximate partitioning algorithms. *Transport. Res. Part C: Emerging Technol.* 133, 103447. doi:10.1016/j.trc.2021.103447.
- Beckmann, M.J., McGuire, C.B., Winsten, C.B., 1956. *Studies in the Economics of Transportation*. Yale University Press, New Haven, Connecticut doi:10.2307/3007560.
- Berman, O., Larson, R.C., Fouska, N., 1992. Optimal location of discretionary service facilities. *Transport. Sci.* 26, 201–211. doi:10.1287/trsc.26.3.201.
- Capar, I., Kuby, M., Leon, V.J., Tsai, Y.J., 2013. An arc cover–path-cover formulation and strategic analysis of alternative-fuel station locations. *Eur. J. Operat. Res.* 227, 142–151. doi:10.1016/j.ejor.2012.11.033.
- Chen, R., Qian, X., Miao, L., Ukkusuri, S.V., 2020. Optimal charging facility location and capacity for electric vehicles considering route choice and charging time equilibrium. *Comput. Operat. Res. Comput. Operat. Res.* 113, 104776. doi:10.1016/j.cor.2019.104776.
- Chen, Z., He, F., Yin, Y., 2016. Optimal deployment of charging lanes for electric vehicles in transportation networks. *Transport. Res. Part B: Methodol.* 91, 344–365. doi:10.1016/j.trb.2016.05.018.
- Chung, B.D., Park, S., Kwon, C., 2018. Equitable distribution of recharging stations for electric vehicles. *Socioecon. Plann. Sci.* 63, 1–11. doi:10.1016/j.seps.2017.06.002.
- Donkers, A., Yang, D., Viktorović, M., 2020. Influence of driving style, infrastructure, weather and traffic on electric vehicle performance. *Transport. Res. Part D: Transport Environ.* 88, 102569. doi:10.1016/j.trd.2020.102569.
- Fakhrmoosavi, F., Kavianiipour, M., Shojaei, M., Zockaie, A., Ghamami, M., Wang, J., Jackson, R., 2021. Electric vehicle charger placement optimization in Michigan considering monthly traffic demand and battery performance variations. *Transport. Res. Record: J. Transport. Res. Board* 2675, 13–29. doi:10.1177/0361198120981958.
- Franke, T., Krems, J.F., 2013. What drives range preferences in electric vehicle users? *Transp. Policy. (Oxf)* 30, 56–62. doi:10.1016/j.tranpol.2013.07.005.
- Ge, Y., MacKenzie, D., 2022. Charging behavior modeling of battery electric vehicle drivers on long-distance trips. *Transport. Res. Part D: Transport Environ.* 113, 103490. doi:10.1016/j.trd.2022.103490.
- Ghamami, M., Kavianiipour, M., Zockaie, A., Hohnstadt, L.R., Ouyang, Y., 2020. Refueling infrastructure planning in intercity networks considering route choice and travel time delay for mixed fleet of electric and conventional vehicles. *Transport. Res. Part C: Emerging Technol.* 120, 102802. doi:10.1016/j.trc.2020.102802.
- Ghamami, M., Zockaie, A., Nie, Y., 2016. A general corridor model for designing plug-in electric vehicle charging infrastructure to support intercity travel. *Transport. Res. Part C: Emerging Technol.* 68, 389–402. doi:10.1016/j.trc.2016.04.016.
- Göpfert, P., Bock, S., 2019. A Branch&Cut approach to recharging and refueling infrastructure planning. *Eur. J. Operat. Res.* 279, 808–823. doi:10.1016/j.ejor.2019.06.031.
- Guo, F., Yang, J., Lu, J., 2018. The battery charging station location problem: Impact of users' range anxiety and distance convenience. *Transport. Res. Part E: Logistic. Transport. Rev.* 114, 1–18. doi:10.1016/j.tre.2018.03.014.
- He, F., Wu, D., Yin, Y., Guan, Y., 2013. Optimal deployment of public charging stations for plug-in hybrid electric vehicles. *Transport. Res. Part B: Methodol.* 47, 87–101. doi:10.1016/j.trb.2012.09.007.
- He, F., Yin, Y., Zhou, J., 2015. Deploying public charging stations for electric vehicles on urban road networks. *Transport. Res. Part C: Emerging Technol.* 60, 227–240. doi:10.1016/j.trc.2015.08.018.
- He, J., Yang, H., Tang, T.-Q., Huang, H.-J., 2018. An optimal charging station location model with the consideration of electric vehicle's driving range. *Transport. Res. Part C: Emerging Technol.* 86, 641–654. doi:10.1016/j.trc.2017.11.026.
- Hodgson, M.J., 1990. A flow-capturing location-allocation model. *Geogr. Anal.* 22, 270–279. doi:10.1111/j.1538-4632.1990.tb00210.x.
- Hodgson, M.J., Rosing, K.E., 1992. A network location-allocation model trading off flow capturing and p-median objectives. *Ann. Oper. Res.* 40, 247–260. doi:10.1007/BF02060480.
- Hodgson, M.J., Rosing, K.E., Storrier, A.L.G., 1996a. Applying the flow-capturing location-allocation model to an authentic network Edmonton, Canada. *Eur. J. Operat. Res.* 90, 427–443. doi:10.1016/0377-2217(95)00034-8.
- Hodgson, M.J., Rosing, K.E., Zhang, J., 1996b. Locating vehicle inspection stations to protect a transportation network. *Geogr. Anal.* 28, 299–314. doi:10.1111/j.1538-4632.1996.tb00937.x.
- Hosseini, M., MirHassani, S.A., 2015. A heuristic algorithm for optimal location of flow-refueling capacitated stations. *Int. Trans. Operat. Res.* 24, 1377–1403. doi:10.1111/itor.12209.
- Hosseini, M., MirHassani, S.A., Hooshmand, F., 2017. Deviation-flow refueling location problem with capacitated facilities: model and algorithm. *Transport. Res. Part D: Transport Environ.* 54, 269–281. doi:10.1016/j.trd.2017.05.015.
- International Energy Agency (2020) Global EV outlook 2020: Entering the decade of electric drive. <https://www.iea.org/reports/global-ev-outlook-2020> [2023-10-18]. Doi: 94399e-en.
- Kassakian, J.G., 2013. Overcoming barriers to electric vehicle deployment: Interim report. *Transport. Res. Board* doi:10.17226/18320.
- Kavianiipour, M., Fakhrmoosavi, F., Shojaei, M., Zockaie, A., Ghamami, M., Wang, J., Jackson, R., 2021. Impacts of technology advancements on electric vehicle charging infrastructure configuration: a Michigan case study. *Int. J. Sustain. Transp.* 16, 597–609. doi:10.1080/15568318.2021.1914789.
- Kchaou-Boujelben, M., 2021. Charging station location problem: a comprehensive review on models and solution approaches. *Transport. Res. Part C: Emerging Technol.* 132, 103376. doi:10.1016/j.trc.2021.103376.
- Kim, J.-G., Kuby, M., 2012. The deviation-flow refueling location model for optimizing a network of refueling stations. *Int. J. Hydrogen. Energy* 37, 5406–5420. doi:10.1016/j.ijhydene.2011.08.108.
- Kim, J.-G., Kuby, M., 2013. A network transformation heuristic approach for the deviation flow refueling location model. *Comput. Operat. Res. Comput. Operat. Res.* 40, 1122–1131. doi:10.1016/j.cor.2012.10.021.
- Kuby, M., Lim, S., 2005. The flow-refueling location problem for alternative-fuel vehicles. *Socioecon. Plann. Sci.* 39, 125–145. doi:10.1016/j.seps.2004.03.001.
- Kuby, M., Lim, S., 2007. Location of alternative-fuel stations using the flow-refueling location model and dispersion of candidate sites on arcs. *Netw. Spat. Econ.* 7, 129–152. doi:10.1007/s1067-006-9003-6.
- Kweon, S.J., Hwang, S.W., Ventura, J.A., 2017. A continuous deviation-flow location problem for an alternative-fuel refueling station on a tree-like transportation network. *J. Adv. Transp.* 1–20. doi:10.1155/2017/1705821, 2017.
- Li, J., Xie, C., Bao, Z., 2022. Optimal en-route charging station locations for electric vehicles: a new modeling perspective and a comparative evaluation of network-based and metanetwork-based approaches. *Transport. Res. Part C: Emerging Technol.* 142, 103781. doi:10.1016/j.trc.2022.103781.
- Li, S., Huang, Y., 2014. Heuristic approaches for the flow-based set covering problem with deviation paths. *Transport. Res. Part E: Logistic. Transport. Rev.* 72, 144–158. doi:10.1016/j.tre.2014.10.013.
- Lim, S., Kuby, M., 2010. Heuristic algorithms for siting alternative-fuel stations using the flow-refueling location model. *Eur. J. Operat. Res.* 204, 51–61. doi:10.1016/j.ejor.2009.09.032.

- Lin, Z., Greene, D.L., 2011. Promoting the market for plug-in hybrid and battery electric vehicles. *Transport. Res. Record: J. Transport. Res. Board* 2252, 49–56. doi:[10.3141/2252-07](https://doi.org/10.3141/2252-07).
- Liu, H., Wang, D.Z.W., 2017. Locating multiple types of charging facilities for battery electric vehicles. *Transport. Res. Part B: Methodol.* 103, 30–55. doi:[10.1016/j.trb.2017.01.005](https://doi.org/10.1016/j.trb.2017.01.005).
- MirHassani, S.A., Ebrazi, R., 2013. A flexible reformulation of the refueling station location problem. *Transport. Sci.* 47, 617–628. doi:[10.1287/trsc.1120.0430](https://doi.org/10.1287/trsc.1120.0430).
- Nourbakhsh, S.M., Ouyang, Y., 2010. Optimal fueling strategies for locomotive fleets in railroad networks. *Transport. Res. Part B: Methodol.* 44, 1104–1114. doi:[10.1016/j.trb.2010.03.003](https://doi.org/10.1016/j.trb.2010.03.003).
- Pearre, N.S., Kempton, W., Guensler, R.L., Elango, V.V., 2011. Electric vehicles: How much range is required for a day's driving? *Transport. Res. Part C: Emerging Technol.* 19, 1171–1184. doi:[10.1016/j.trc.2010.12.010](https://doi.org/10.1016/j.trc.2010.12.010).
- Riemann, R., Wang, D.Z.W., Busch, F., 2015. Optimal location of wireless charging facilities for electric vehicles: Flow-capturing location model with stochastic user equilibrium. *Transport. Res. Part C: Emerging Technol.* 58, 1–12. doi:[10.1016/j.trc.2015.06.022](https://doi.org/10.1016/j.trc.2015.06.022).
- Rose, P.K., Nugroho, R., Gnann, T., Plötz, P., Wietschel, M., Reuter-Oppermann, M., 2020. Optimal development of alternative fuel station networks considering node capacity restrictions. *Transport. Res. Part D: Transport Environ.* 78, 102189. doi:[10.1016/j.trd.2019.11.018](https://doi.org/10.1016/j.trd.2019.11.018).
- Shen, Z.-J.M., Feng, B., Mao, C., Ran, L., 2019. Optimization models for electric vehicle service operations: a literature review. *Transport. Res. Part B: Methodol.* 128, 462–477. doi:[10.1016/j.trb.2019.08.006](https://doi.org/10.1016/j.trb.2019.08.006).
- Shi, X., Pan, J., Wang, H., Cai, H., 2019. Battery electric vehicles: What is the minimum range required? *Energy* 166, 352–358. doi:[10.1016/j.energy.2018.10.056](https://doi.org/10.1016/j.energy.2018.10.056).
- Stark, J., Link, C., Simic, D., Bäuml, T., 2015. Required range of electric vehicles – an analysis of longitudinal mobility data. *IET Intell. Transport Syst.* 9, 119–127. doi:[10.1049/iet-its.2013.0019](https://doi.org/10.1049/iet-its.2013.0019).
- Tran, T.H., Nagy, G., Nguyen, T.B.T., Wassan, N.A., 2018. An efficient heuristic algorithm for the alternative-fuel station location problem. *Eur. J. Operat. Res.* 269, 159–170. doi:[10.1016/j.ejor.2017.10.012](https://doi.org/10.1016/j.ejor.2017.10.012).
- Upchurch, C., Kuby, M., Lim, S., 2009. A model for location of capacitated alternative-fuel stations. *Geogr. Anal.* 41, 85–106. doi:[10.1111/j.1538-4632.2009.00744.x](https://doi.org/10.1111/j.1538-4632.2009.00744.x).
- U.S. Bureau of Public Roads, 1964. *Traffic assignment manual for application with a large, high speed computer*. Bureau of Public Roads, U.S. Department of Commerce, Washington D.C.
- Ventura, J.A., Kweon, S.J., Hwang, S.W., Tormay, M., Li, C., 2017. Energy policy considerations in the design of an alternative-fuel refueling infrastructure to reduce GHG emissions on a transportation network. *Energy Policy* 111, 427–439. doi:[10.1016/j.enpol.2017.09.035](https://doi.org/10.1016/j.enpol.2017.09.035).
- Wang, C., He, F., Lin, X., Shen, Z.-J.M., Li, M., 2019a. Designing locations and capacities for charging stations to support intercity travel of electric vehicles: An expanded network approach. *Transport. Res. Part C: Emerging Technol.* 102, 210–232. doi:[10.1016/j.trc.2019.03.013](https://doi.org/10.1016/j.trc.2019.03.013).
- Wang, X., Shahidepour, M., Jiang, C., Li, Z., 2019b. Coordinated planning strategy for electric vehicle charging stations and coupled traffic-electric networks. *IEEE Trans. Power Syst.* 34, 268–279. doi:[10.1109/tpwrs.2018.2867176](https://doi.org/10.1109/tpwrs.2018.2867176).
- Wang, X., Song, Z., Xu, H., Wang, H., 2023. En-route fast charging infrastructure planning and scheduling for battery electric bus systems. *Transport. Res. Part D: Transport Environ.* 117, 103659. doi:[10.1016/j.trd.2023.103659](https://doi.org/10.1016/j.trd.2023.103659).
- Wang, Y.-W., 2007. An optimal location choice model for recreation-oriented scooter recharge stations. *Transport. Res. Part D: Transport Environ.* 12, 231–237. doi:[10.1016/j.trd.2007.02.002](https://doi.org/10.1016/j.trd.2007.02.002).
- Wang, Y.-W., Lin, C.-C., 2009. Locating road-vehicle refueling stations. *Transport. Res. Part E: Logistic. Transport. Rev.* 45, 821–829. doi:[10.1016/j.tre.2009.03.002](https://doi.org/10.1016/j.tre.2009.03.002).
- Wang, Y.-W., Lin, C.-C., 2013. Locating multiple types of recharging stations for battery-powered electric vehicle transport. *Transport. Res. Part E: Logistic. Transport. Rev.* 58, 76–87. doi:[10.1016/j.tre.2013.07.003](https://doi.org/10.1016/j.tre.2013.07.003).
- Wang, Y., Shi, J., Wang, R., Liu, Z., Wang, L., 2018. Siting and sizing of fast charging stations in highway network with budget constraint. *Appl. Energy* 228, 1255–1271. doi:[10.1016/j.apenergy.2018.07.025](https://doi.org/10.1016/j.apenergy.2018.07.025).
- Xie, C., Jiang, N., 2016. Relay requirement and traffic assignment of electric vehicles. *Comput.-Aided Civil Infrastruct. Eng.* 31, 580–598. doi:[10.1111/mice.12193](https://doi.org/10.1111/mice.12193).
- Xie, C., Wang, T.-G., Pu, X., Karoonsontawong, A., 2017. Path-constrained traffic assignment: Modeling and computing network impacts of stochastic range anxiety. *Transport. Res. Part B: Methodol.* 103, 136–157. doi:[10.1016/j.trb.2017.04.018](https://doi.org/10.1016/j.trb.2017.04.018).
- Xu, M., Meng, Q., 2020. Optimal deployment of charging stations considering path deviation and nonlinear elastic demand. *Transport. Res. Part B: Methodol.* 135, 120–142. doi:[10.1016/j.trb.2020.03.001](https://doi.org/10.1016/j.trb.2020.03.001).
- Xu, M., Yang, H., Wang, S., 2020. Mitigate the range anxiety: Siting battery charging stations for electric vehicle drivers. *Transport. Res. Part C: Emerging Technol.* 114, 164–188. doi:[10.1016/j.trc.2020.02.001](https://doi.org/10.1016/j.trc.2020.02.001).
- Xylia, M., Leduc, S., Patrizio, P., Kraxner, F., Silveira, S., 2017. Locating charging infrastructure for electric buses in Stockholm. *Transport. Res. Part C: Emerging Technol.* 78, 183–200. doi:[10.1016/j.trc.2017.03.005](https://doi.org/10.1016/j.trc.2017.03.005).
- Yildiz, B., Arslan, O., Karasan, O.E., 2016. A branch and price approach for routing and refueling station location model. *Eur. J. Operat. Res.* 248, 815–826. doi:[10.1016/j.ejor.2015.05.021](https://doi.org/10.1016/j.ejor.2015.05.021).
- Zeng, X., Xie, C., Xu, M., Chen, Z., 2024. Optimal en-route charging station locations for electric vehicles with heterogeneous range anxiety. *Transport. Res. Part C: Emerging Technol.* 158, 104459. doi:[10.1016/j.trc.2023.104459](https://doi.org/10.1016/j.trc.2023.104459).
- Zhang, H., Moura, S.J., Hu, Z., Song, Y., 2018a. PEV fast-charging station siting and sizing on coupled transportation and power networks. *IEEE Trans. Smart. Grid.* 9, 2595–2605. doi:[10.1109/tsg.2016.2614939](https://doi.org/10.1109/tsg.2016.2614939).
- Zhang, L., Shaffer, B., Brown, T., Scott Samuelsen, G., 2015. The optimization of DC fast charging deployment in California. *Appl. Energy* 157, 111–122. doi:[10.1016/j.apenergy.2015.07.057](https://doi.org/10.1016/j.apenergy.2015.07.057).
- Zhang, X., Rey, D., Waller, S.T., 2018b. Multitype recharge facility location for electric vehicles. *Computer-Aided Civil Infrastruct. Eng.* 33, 943–965. doi:[10.1111/mice.12379](https://doi.org/10.1111/mice.12379).
- Zheng, H., He, X., Li, Y., Peeta, S., 2017. Traffic equilibrium and charging facility locations for electric vehicles. *Netw. Spat. Econ.* 17, 435–457. doi:[10.1007/s11067-016-9332-z](https://doi.org/10.1007/s11067-016-9332-z).
- Zheng, H., Peeta, S., 2017. Routing and charging locations for electric vehicles for intercity trips. *Transport. Plann. Technol.* 40, 393–419. doi:[10.1080/03081060.2017.1300245](https://doi.org/10.1080/03081060.2017.1300245).